

Water Resources Research®

RESEARCH ARTICLE

10.1029/2021WR030852

Key Points:

- Remote time-lapse cameras and citizen science shed light on forest-snow interception processes that are often overlooked
- Site specific interception patterns, such as wind dominated unloading and riming, impact the transferability of unloading parameterizations
- The choice of unloading scheme impacts the canopy albedo feedback, and the partitioning of snow on the ground versus canopy sublimation

Supporting Information:

Supporting Information may be found in the online version of this article.

Correspondence to:

C. Lumbrazo,
lumbraca@uw.edu

Citation:






Lumbrazo, C., Bennett, A., Currier, W. R., Nijssen, B., & Lundquist, J. (2022). Evaluating multiple canopy-snow unloading parameterizations in SUMMA with time-lapse photography characterized by citizen scientists. *Water Resources Research*, 58, e2021WR030852. <https://doi.org/10.1029/2021WR030852>

Received 30 JUL 2021
Accepted 10 MAY 2022

Author Contributions:

Conceptualization: Cassie Lumbrazo, Bart Nijssen, Jessica Lundquist
Data curation: William Ryan Currier
Formal analysis: Cassie Lumbrazo, Andrew Bennett, William Ryan Currier
Funding acquisition: Jessica Lundquist
Investigation: Cassie Lumbrazo
Methodology: Cassie Lumbrazo, Andrew Bennett, Jessica Lundquist
Project Administration: Jessica Lundquist
Resources: William Ryan Currier, Bart Nijssen
Software: Cassie Lumbrazo, Andrew Bennett
Supervision: Bart Nijssen, Jessica Lundquist
Validation: Cassie Lumbrazo

Evaluating Multiple Canopy-Snow Unloading Parameterizations in SUMMA With Time-Lapse Photography Characterized by Citizen Scientists

Cassie Lumbrazo¹ , Andrew Bennett¹ , William Ryan Currier^{1,2} , Bart Nijssen¹ , and Jessica Lundquist¹ 

¹Department of Civil and Environmental Engineering, University of Washington, Seattle, WA, USA, ²Earth System Research Laboratory, Physical Science Laboratory, National Oceanic and Atmospheric Administration, Boulder, CO, USA

Abstract Canopy-snow unloading is the complex physical process of snow unloading from the canopy through meltwater drip, sublimation to the atmosphere, or solid snow unloading to the snowpack below. This process is difficult to parameterize due to limited observations. Time-lapse photographs of snow in the canopy were characterized by citizen scientists to create a data set of snow interception observations at multiple locations across the western United States. This novel interception data set was used to evaluate three snow unloading parameterizations in the Structure for Unifying Multiple Modeling Alternatives (SUMMA) modular hydrologic modeling framework. SUMMA was modified to include a third snow unloading parameterization, termed Wind-Temperature (Roesch et al., 2001, <https://doi.org/10.1007/s003820100153>), which includes wind-dependent and temperature-dependent unloading functions. It was compared to a meltwater drip unloading parameterization, termed Melt (Andreadis et al., 2009, <https://doi.org/10.1029/2008wr007042>), and a time-dependent unloading parameterization, termed Exponential-Decay (Hedstrom & Pomeroy, 1998, [https://doi.org/10.1002/\(SICI\)1099-1085\(199808/09\)12:10/11<1611::AID-HYP684>3.0.CO;2-4](https://doi.org/10.1002/(SICI)1099-1085(199808/09)12:10/11<1611::AID-HYP684>3.0.CO;2-4)). Wind-Temperature performed well without calibration across sites, specifically in cold climates, where wind dominates unloading and rime accretion is low. At rime prone sites, Wind-Temperature should be calibrated to account for longer interception events with less sensitivity to wind, otherwise Melt can be used without calibration. The absence of model physics in Exponential-Decay requires local calibration that can only be transferred to sites with similar unloading patterns. The choice of unloading parameterization can result in 20% difference in SWE on the ground below the canopy and 10% difference in estimated average winter canopy albedo. These novel observations shed light on processes that are often overlooked in hydrology.

Plain Language Summary Forests intercept snowfall and affect how much snow accumulates on the landscape. Canopy snow can unload by melting onto the snowpack below, sublimating back to the atmosphere, or by sluffing off and contributing to the ground's snowpack. It has been difficult to create and validate models for canopy-snow unloading due to limited observations. However, time-lapse photography can observe canopy-snow unloading in remote areas. In this work, these were characterized by citizen scientists to create an observational data set of snow interception, which we used to evaluate the performance of three canopy-snow unloading models. Models that unloaded snow as a function of wind and temperature performed better than time-based estimates. How a model unloads snow impacts the model's estimate of water available for runoff because it changes how much intercepted snow is modeled as falling to the ground versus lost back to the atmosphere. Additionally, different models of how long snow stays in the canopy impact the models' estimates of how much radiation was reflected back to the atmosphere. This work shows that citizen scientists can substantially contribute to science and produce a novel data set that can be used to investigate processes often overlooked in hydrology.

1. Introduction

Forest covers a significant portion of the Northern Hemisphere land surface and 40% of the North American snow zone (Klein et al., 1998). Depending on the climate, needleleaf coniferous forests can intercept 30–80% of a storm's snowfall (Hedstrom & Pomeroy, 1998; Lundquist et al., 2013; Martin et al., 2013; Storck, 2000). Sublimation of the snow in the canopy is a significant component of the water balance (Essery et al., 2003), and in certain cases, losses associated with canopy sublimation can exceed 30% (Molotch et al., 2007; Montesi et al., 2004).

Visualization: Cassie Lumbrazo, William Ryan Currier

Writing – original draft: Cassie Lumbrazo

Writing – review & editing: Cassie Lumbrazo, Andrew Bennett, William Ryan Currier, Bart Nijssen, Jessica Lundquist

In addition, the physical process of forest-snow interception has a large influence on the land surface energy balance for these regions (Essery, 1998). Dense coniferous forests naturally have a low albedo. Once the evergreen canopy is covered with snow, the albedo of the entire land surface increases by about 20% (Webster & Jonas, 2018) along with its energy feedback to the atmosphere (Thackeray et al., 2014). Although it is known that global climate models are particularly sensitive to the snow and ice albedo feedback, many still have poorly simulated land surface schemes for the winter albedo of a boreal forest (Bartlett & Verseghy, 2015; Bonan et al., 1992). Studies show that properly representing the physical processes involved in canopy interception can improve the simulated surface albedo over boreal forest regions (Niu & Yang, 2004).

To properly represent the albedo over forested areas, it is critically important to resolve the timing of snow unloading from the canopy once it is intercepted. While often overlooked, snow unloading is a complex physical process. Once snow accumulates in the canopy, it can melt out as water dripping onto the snowpack below, unload as snow from the canopy onto the snowpack below, or sublimate back to the atmosphere (Lundquist et al., 2021). Additional complexity is added when rime ice forms on the canopy, impacting the physical properties of the intercepted snow (Whiteman & Garibotti, 2013). Snow unloading through these mechanisms often results in a large, and sometimes sudden, decrease in land surface albedo. In addition, this complex process is difficult to parametrize due to limited observations, making existing model formulations difficult to evaluate (Lundquist et al., 2021). Thus, the goal of this work is to evaluate the performance of three widely used canopy-snow-unloading parameterizations, using a modular snow model that holds all other processes constant, combined with time-lapse photographs from several climates, interpreted by citizen scientists.

The three unloading parameterizations include, (a) snow leaves the canopy along with meltwater drip (Andreadis et al., 2009), (b) snow unloads from the canopy according to an exponential decay rate as a function of time after an interception event (Hedstrom & Pomeroy, 1998), and (c) snow unloads as a function of both temperature and wind, each bound by minimum constraints (Roesch et al., 2001; Table 1).

For the remainder of this paper, the Andreadis et al. (2009) canopy-snow unloading parameterization will be referred to as Melt unloading, Hedstrom and Pomeroy (1998) as Exponential-Decay unloading, and Roesch et al. (2001) as Wind-Temperature unloading (Table 1).

The three canopy-snow parameterizations are calibrated and evaluated using time-lapse photography of forest-snow interception at four sites to answer the following research questions:

1. How well do these unloading parameterizations work in different environments with,
 - (a) default parameter values?
 - (b) locally calibrated parameter values?
 - or (c) parameter values calibrated and transferred to a different site?
2. What factors lead to model differences?
3. How does our choice of unloading impact the modeled fate of snow in the canopy?

This paper is arranged as follows: Section 2 describes the study sites and model forcing data, Section 3 provides information about the novel observational data set of forest-snow interception created by citizen scientists from time-lapse photography; it also outlines the three unloading parameterizations, explains model calibration, and the evaluation process. Section 4 answers the research questions, while Section 5 discusses the albedo implications of the different parameterizations and physical processes missing from the existing models. Finally, we provide conclusions and some remarks on future research in Section 6.

2. Study Sites and Forcing Data

We evaluated the snow unloading parameterizations at four different locations: Niwot Ridge, CO, Mount Hopper, WA, and Mesa West and LSOS on Grand Mesa, CO (Figure 1).

2.1. Niwot Ridge, CO

Niwot Ridge is located at 3,050 m elevation on the leeward side of the Continental Divide in Colorado, USA, and has a cold continental climate. This site is windy, with 7–8 m tall mixed subalpine fir (*Abies lasiocarpa*), Engelmann spruce (*Picea engelmannii*), and lodgepole pine (*Pinus contorta*) that create a dense coniferous forest.

Table 1
Canopy-Snow Unloading Parametrizations

Unloading parameterization citation	Short name	Parameterization unloading process
Andreadis et al. (2009)	Melt	Solid snow in the canopy unloads in the presence of meltwater drip
Hedstrom and Pomeroy (1998)	Exponential-Decay	Time-dependent exponential decay unloading
Roesch et al. (2001)	Wind-Temperature	Wind-dependent and temperature-dependent unloading

Time-lapse photos were taken every 30 min on the Ameriflux Tower, above the canopy, and were archived by the PhenoCam Network (Milliman et al., 2018).

Hourly forcing data for water year (WY; 1 October to 30 September) 2017 were collected from the onsite Ameriflux Meteorological Tower (Ameriflux Site US-NR1) at a 20 m measurement height and also extracted from the High-Resolution Rapid Refresh (HRRR) atmospheric model (Horel & Blaylock, 2019) at 3-km spatial resolution. HRRR simulates winds for the lowest level of the atmosphere, 50 m above the ground, through a Navier Stokes Solution, then calculates the 10-m wind speed by interpolating to a height of 10 m, assuming a logarithmic profile for the wind speed.

Ameriflux data for winter (1 November–1 April) in WY 2017 showed a mean temperature of -4.4°C , mean wind speed of 6.8 m s^{-1} , reaching up to a maximum hourly average of 21.6 m s^{-1} , and a total precipitation of 1,420 mm. For the same period and location, HRRR data showed a mean temperature of -3.9°C , mean wind-speed of 7.5 m s^{-1} , reaching up to a maximum hourly average of 27.1 m s^{-1} , and a total precipitation of 1,342 mm (Table 2). Because HRRR data matched well with observations at Niwot Ridge, CO we assumed this as a reasonable data set to use at Grand Mesa, CO as well.

2.2. Mount Hopper, WA

Mount Hopper is a warm and wet maritime site, located in Olympic National Park in Washington State, USA at an elevation of 1,864 m in a dense coniferous forest mostly consisting of 20–30 m tall western hemlock (*Tsuga heterophylla*) and mountain hemlock (*Tsuga mertensiana*), with some smaller subalpine fir (*A. lasiocarpa*). The interception observations are from time-lapse photos taken every 3 hr, during daylight hours, as a part of the OLYMPEX ground validation campaign during WY 2016 (Kim et al., 2017).

The unloading parameterizations were tested using forcing data for WY 2016 from the Weather Research and Forecasting (WRF) Model (Skamarock et al., 2008) at 4/3-km spatial resolution, provided by the Northwest Modeling Consortium (Mass et al., 2003). WRF output was used because HRRR was not archived before WY 2017. These WRF data are at a higher spatial resolution than HRRR and were specifically evaluated during the OLYMPEX campaign (Currier et al., 2017). When these data were used to force a hydrologic model, they produced unbiased estimates of peak SWE and captured the timing and magnitude of snowfall events during the accumulation season (Currier et al., 2017). Both WRF and HRRR simulations used the Thompson et al. (2008) microphysical scheme without convective parameterizations. Incoming shortwave and longwave radiation used the Rapid Radiative Transfer Model (Mlawer et al., 1997). WRF data at Mount Hopper for the winter (1 November to 1 April) in WY 2016 showed a mean air temperature of -1.6°C , a mean wind speed of 5.8 m s^{-1} , reaching up to an hourly average of 27.2 m s^{-1} , and total precipitation of 2,409 mm (Table 2).

2.3. Mesa West (MW) and LSOS, Grand Mesa, CO

Two evaluation sites were on Grand Mesa in Colorado, USA, where NASA's 2017 SnowEx Field Campaign took place. Grand Mesa had similar mean winter temperature and wind speeds to Niwot Ridge.

The Mesa West (MW) site is an exposed and windy location on the west end of the mesa at 3,033 m with 5–6 m tall Engelmann spruce (*P. engelmannii*) and subalpine fir (*A. lasiocarpa*) coniferous trees organized into densely forested patches on the mesa from constant wind exposure. HRRR data for the winter (1 November to 1 April) in WY 2017 showed a mean temperature of -4.5°C , mean wind speed of 6.6 m s^{-1} , reaching up to a maximum hourly average of 23.8 m s^{-1} , and a total precipitation of 1,274 mm. In contrast, the Local Scale Observational Site (LSOS) is located just off and north of the mesa at 2,974 m with mixed 7–8 m lodgepole pine (*Pinus cortorta*) and

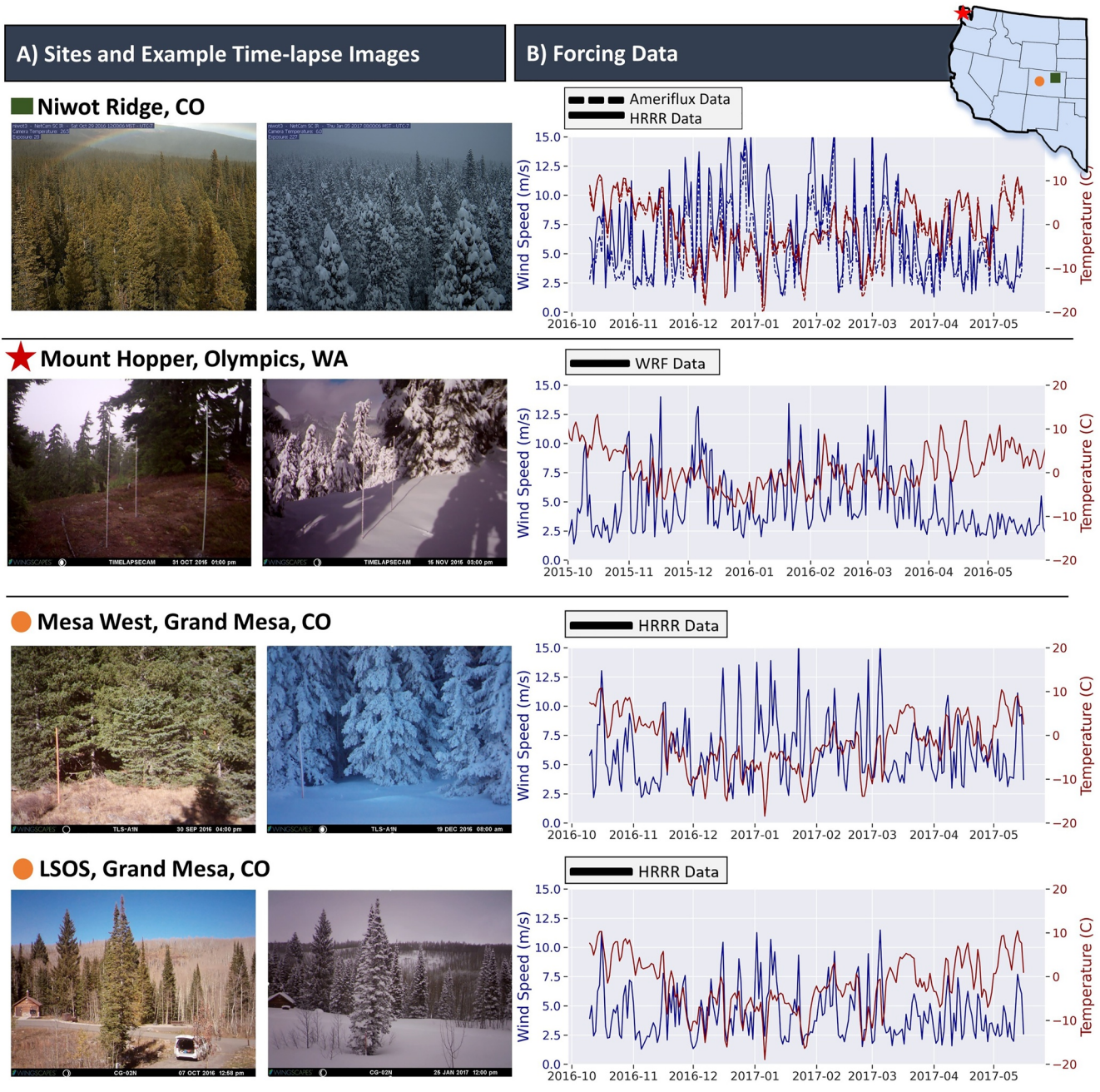


Figure 1. (a) Study sites and example time-lapse images, with and without snow present in the canopy. Marker colors correspond with the western United States map (upper right) for Niwot Ridge, CO (green square), Mount Hopper in Olympic National Park, WA (red star), and Mesa West (MW) and LSOS on Grand Mesa, CO (orange circle). (b) Time series of windspeed (m s^{-1} , solid blue line on left axis) and temperature ($^{\circ}\text{C}$, solid red line on right axis) from the Ameriflux, High-Resolution Rapid Refresh (HRRR), and Weather Research and Forecasting (WRF) forcing data used for each site.

smaller aspen (*Populus tremuloides*) trees that create an evenly distributed, less dense forest structure in comparison to Mesa West. LSOS had a mean winter temperature of -4.8°C , mean wind speed of 4.5 m s^{-1} , reaching up to a maximum hourly average of 16.1 m s^{-1} , and a total precipitation of 1,876 mm for the same data set and timeframe as Mesa West (Table 2). While there are meteorological stations available at each site, environmental conditions, high winds, and air temperatures between -2 and -8°C (Whiteman & Garibotti, 2013), make them subject to riming, resulting in inaccurate periods of zeros for wind speed because of ice on the anemometers through the winter months. Thus, forcing data for both sites were taken from HRRR for WY 2017. Time-lapse

Table 2
Site, Water Year (WY), Data Source, and Forcing Data Means and Totals Calculated Between 1 November and 1 April

Model site	WY	Data source	Mean temp (°C)	Mean wind (m s ⁻¹)	Total precip (mm)	Mean RH (%)
Niwot Ridge, CO	2017	Ameriflux	-4.4	6.8	1,420	63.8
Niwot Ridge, CO	2017	HRRR	-3.9	7.5	1,342	60.1
Mount Hopper, WA	2016	WRF	-1.6	5.8	2,409	91.7
Mesa West, CO	2017	HRRR	-4.5	6.6	1,274	71.9
LSOS, CO	2017	HRRR	-4.8	4.5	1,876	70.3

photos were taken five times per day at both sites, providing interception observations approximately every 2 hr during daylight hours.

3. Methods

3.1. Citizen Science Observations of Canopy-Snow Interception

Modeling snow interception and unloading is difficult due to complex forest-snow interactions that limit the ability to conduct experiments in the field and in a laboratory environment. Lundquist et al. (2021) outlines previous field experiments that form the foundation for existing models, such as branches clipped to a pole (Schmidt & Gluns, 1991) and two Douglas Fir trees mounted on weighing lysimeters (Storck, 2000). These methods are often expensive, time-consuming, and not reproducible in different environments, which leads to uncertainty in the resulting empirical approximations.

Time-lapse photography is a unique tool that can capture forest-snow processes in remote areas and adverse weather conditions. Time-lapse images from high-resolution digital cameras were collected from the PhenoCam Network (Milliman et al., 2018), the 2017 NASA SnowEx Field Campaign (Currier et al., 2019; Kim et al., 2017; Raleigh et al., 2022), and the Olympic Mountain Experiment (OLYMPEX) ground validation campaign (Currier et al., 2017; Houze et al., 2017; Lundquist et al., 2018). These images were then uploaded to a citizen science platform called Zooniverse (Zooniverse.org) and classified by thousands of volunteers as part of the *Snow Spotter* project (Figure 2).

The goal of Snow Spotter was to mobilize citizen scientists to quantify information about canopy interception. A total of 6,700 volunteer citizen scientists responded to questions about 13,600 images from sites across the United States. The interested reader is referred to the complete data set (Lumbrazo et al., 2022), but for the scope of this work just one question at four sites was used. The question that provided the most quantitative information for this research was, “Is there snow in the tree branches?” where citizen scientists could respond *Yes*, *No*, or *Unsure*, to photos of a site presented in a random order (Figure 2a). Volunteers provided 9–15 classifications per image and agreed 95–98% of the time on the classification, depending on the site. All classifications for a single image were averaged, and if more than half of the volunteers agreed that there was snow in the trees, then it was recorded as snow present in the final data set; otherwise, it was recorded as no snow present. For a site with more than one time-lapse image taken per hour, such as Niwot Ridge, all the responses within an hour were averaged to create one binary datapoint per hour.

This unique data set provided a look into how canopy interception differs at sites in different climates (e.g., Niwot Ridge compared to Mount Hopper) and at sites that are in the same climate, but with different local topography that impact interception (e.g., Mesa West compared to LSOS). Niwot Ridge had a pattern of frequent yet short interception events, due to high wind speeds that lead to unloading in a cold, dry climate. In contrast, Mount Hopper had long interception events that occurred from either constant precipitation or temperatures that hovered right around freezing, which caused a melt-freeze cycle to firmly attach snow to the canopy. While Mesa West and LSOS are physically close in distance, the local topography of Mesa West led to longer interception events than LSOS, due to high wind speeds at Mesa West that carried saturated air over the mesa and formed rime in the canopy (Figure 2b).

3.2. Modeling Canopy-Snow Unloading Parameterizations in SUMMA

Three widely used canopy-snow unloading parameterizations were evaluated within a modular hydrologic modeling framework, the Structure for Unifying Multiple Modeling Alternatives, SUMMA (Clark et al., 2015a, 2015b, 2015c), by comparing model results with the snow interception time series described in Section 3.1. We updated SUMMA to include a third unloading scheme, Wind-Temperature unloading (Roesch et al., 2001) (Table 1), which is now available in SUMMA Version 3 (Clark et al., 2020). The other two unloading schemes are Exponential-Decay unloading and Melt unloading (Table 1). Since SUMMA is a modular modeling framework, it has the capability of evaluating each unloading parameterization independently, while keeping all other model process parameterizations and parameters constant.

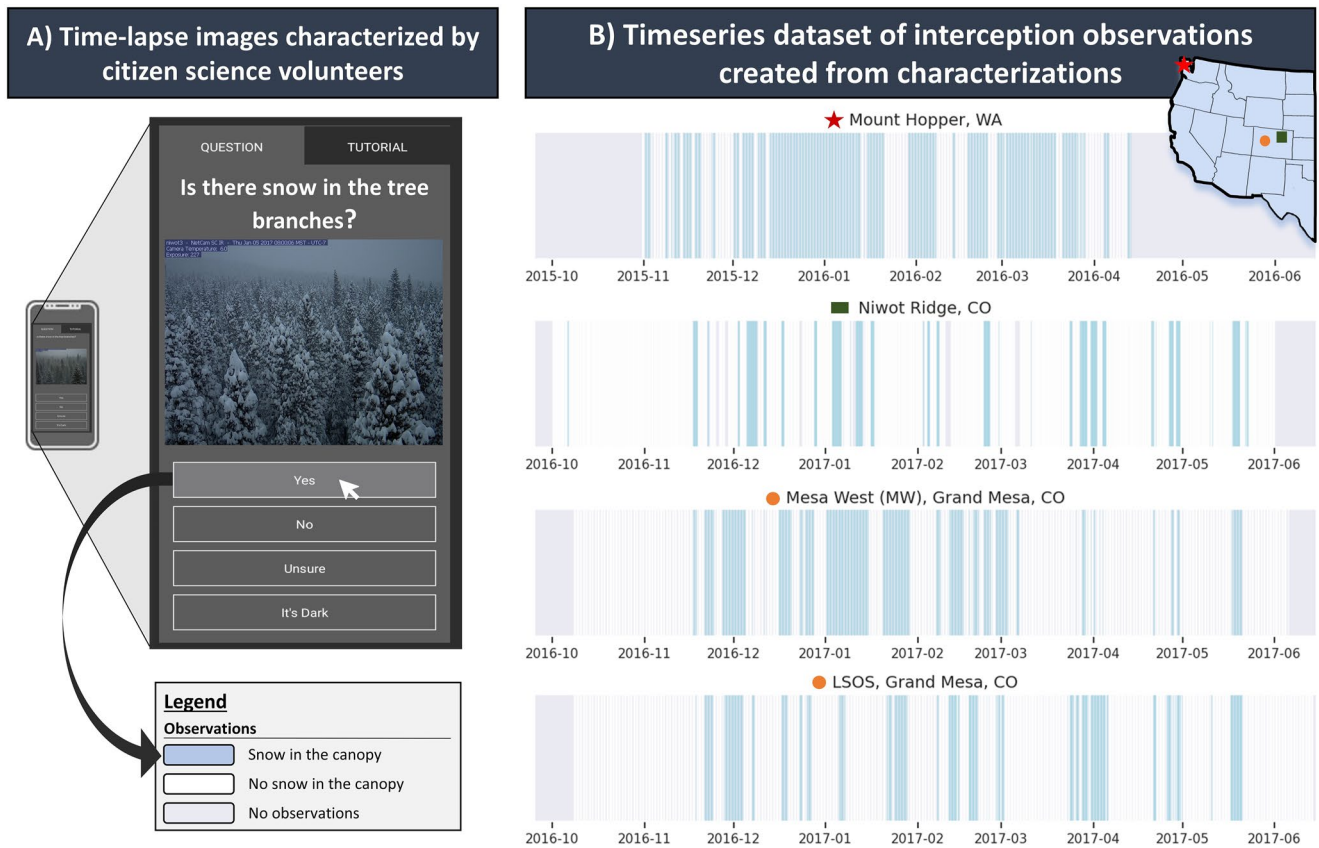


Figure 2. (a) Time-lapse images were collected for each site and uploaded to the citizen science platform, Zooniverse, where online volunteers responded to several questions about snow in the canopy (i.e., Is there snow in the tree branches?). (b) The processed data set for each site, where the marker colors correspond with the western United States map (upper right), for Mount Hopper in Olympic National Park, WA (red star), Niwot Ridge, CO (green square), and Mesa West (MW) and LSOS on Grand Mesa, CO (orange circle). Binary interception observations are represented by the vertical shadings, where blue represents response “Yes,” snow in the canopy, white represents “No,” no snow in the canopy, and gray represents no observations from missing or dark time-lapse images.

Snow and liquid water unloading from the canopy, U ($\text{kg m}^{-2} \text{s}^{-1}$) is only one piece of a system of equations which determines the snow water equivalent, SWE_C , in the canopy at any specified time step. The evolution of intercepted snow in the canopy, I_s , in kg per unit area of vegetation, is defined as

$$\frac{dI_s}{dt} = P - E - U \quad (1)$$

where P ($\text{kg m}^{-2} \text{s}^{-1}$) is the rate of precipitation as snow that is intercepted and E ($\text{kg m}^{-2} \text{s}^{-1}$) is the mass loss from sublimation and gain from rime deposition.

Canopy sublimation is calculated in SUMMA as a flux from the canopy to the canopy air space, dependent of the gradient between the air vapor pressure and the saturation vapor pressure at the canopy temperature. The interested reader is referred to Equations 54, 61, and 68 in the SUMMA technical note (Clark et al., 2015c).

Snow and liquid water unloading from the canopy, U , can be described as

$$U = U_s + U_m \quad (2)$$

where U_s ($\text{kg m}^{-2} \text{s}^{-1}$) represents solid snow unloading and sluffing off the canopy as a mass, contributing to the snowpack below the canopy, and U_m ($\text{kg m}^{-2} \text{s}^{-1}$) represents snow melting within the canopy and dripping onto the snowpack below.

In this work, only parameterizations directly impacting U are evaluated, while parameterizations impacting all other physical processes remain unchanged. Independent of the canopy-snow unloading parameterizations, liquid

Table 3
Default and Locally Calibrated Parameter Values for Each Canopy-Snow Unloading Parameterization

Model parameter and unloading scheme	Min, max, default, and locally calibrated parameter values for each site						
	Min	Max	Default	Niwot Ridge	Mount Hopper	Mesa West	LSOS
Melt							
Ratio of melt drip, r (ratio)	0.0	1.0	0.4	-	-	-	-
Exponential-Decay							
Coefficient of unload, k (s^{-1})	0.0	2.0E-7	6.4E-4	1.5E-5	3.8E-7	2.0E-6	4.0E-6
Corresponding e -folding time (days)	Never	22	0.02	0.33	11.8	2.25	1.12
Wind-Temperature							
Wind empirical constant, C_v (K s)	1.0E5	1.0E8	1.56E5	1.0E5	3.0E7	1.5E6	4.5E5
Minimum wind, v_m ($m\ s^{-1}$)	0.0	10.0	5.0	-	-	-	-
Minimum temperature, T_m (K)	260.16	273.16	270.15	-	-	-	-
Temperature empirical constant, C_T (m)	1.0E5	3.0E5	1.87E5	-	-	-	-

Note. Parameters kept fixed at the default are marked with “-”.

water will drip out of the canopy above a maximum liquid water holding capacity. This is calculated separately from the unloading schemes, and each snow unloading scheme relates to this liquid water drip in a different way. Melt unloading uses liquid water drip as an input, Exponential-Decay unloading is independent of liquid water drip, and Wind-Temperature unloading is indirectly related to it through temperature.

While all other process parameterizations and parameters in SUMMA were left unchanged, changes in U impact the overall $SWEC$. As a result, evaporation, transpiration, and sublimation from the canopy varied between SUMMA simulations that used different unloading parameterizations. For the specific SUMMA model setup, model decisions and model parameters used in this paper, see Tables S3 and S4 in Supporting Information S1, respectively.

3.2.1. Melt Unloading (Andreadis et al., 2009)

The first unloading parameterization evaluated, termed Melt unloading (Table 1), is based on fieldwork by Storck (2000) and is documented in Andreadis et al. (2009). It was developed in a maritime climate with frequent midwinter melt and high snow densities. Melt unloading represents snow unloading from the canopy, U_s , as

$$U_s = 0, \quad \text{for } L_c \leq L_m,$$

$$U_s = r \cdot U_m, \quad \text{for } L_c > L_m, \quad (3)$$

where L_c ($kg\ m^{-2}$) is liquid water accumulating on the canopy, and L_m ($kg\ m^{-2}$) is the maximum liquid water storage before canopy drainage begins. U_m ($kg\ m^{-2}\ s^{-1}$; Equation 2) is the canopy liquid drainage flux of liquid water draining from the vegetation canopy, and r is the ratio of solid snow that unloads from the canopy to the snowpack below, once the liquid water storage in the canopy has been exceeded. Storck et al. (2002) observed unloading when air temperatures were above $0^\circ C$ in the maritime climate of Umpqua, Oregon and found that the ratio, r (Equation 3), of solid to melted snow was approximately 40%. In SUMMA, r is a tunable parameter with a default value of 0.4, but it can be set anywhere in the range of 0–1 (Table 3).

3.2.2. Exponential-Decay Unloading (Hedstrom & Pomeroy, 1998)

The second unloading parameterization, termed Exponential-Decay unloading (Table 1), uses an exponential decay function to unload a mass of snow from the canopy as a function of time, t , to the snow beneath the canopy. This parameterization, formulated in Hedstrom and Pomeroy (1998), was developed in a continental climate with cold winters and low snow densities. Exponential-Decay unloading defines the rate of snow unloading from the canopy, U_s , as

$$U_s = \frac{dI_s}{dt} = -kI_s, \quad (4)$$

where k (s^{-1}) is the coefficient of unloading, and I_s ($kg\ m^{-2}$) is the intercepted snow in the canopy. Integrating Equation 4 provides an exponential decay in intercepted snow over time, t ,

$$I_s = I_0 (e^{-kt}), \quad (5)$$

where I_0 ($kg\ m^{-2}$) is the intercepted snow load at the start of unloading. In the Exponential-Decay parameterization, solid snow unloading from the canopy, U_s , is not related to the occurrence of melt within the canopy. The coefficient of unloading, k , is a tunable parameter in SUMMA (Table S4 in Supporting Information S1). As reported in Gelfan et al. (2004), the value of Hedstrom and Pomeroy's (1998) k is $6.467 \times 10^{-4}\ s^{-1}$, which corresponds to an e -folding time, the time for a quantity to decrease by a factor of e , of less than an hour. As detailed in Supporting Information S1, the original paper does not provide a clear estimate for k but indicates that it may be between 6.4×10^{-7} and $4.5 \times 10^{-6}\ s^{-1}$, corresponding to e -folding times of 7 to 1 day(s), respectively (Section S1.1 in Supporting Information S1). We used Gelfan's value as the default value since it is the only value explicitly written in the literature and is frequently used, but we tested a wide range of k values, up to $k = 2.0E-7\ s^{-1}$, corresponding to 22 days e -folding time, recognizing the uncertainty in this parameter (Table 3).

3.2.3. Wind-Temperature Unloading (Roesch et al., 2001)

The third unloading parameterization, termed Wind-Temperature unloading (Table 1), is formulated in Roesch et al. (2001), who wanted a better way to represent the albedo over forests and created a snow unloading scheme that is both wind and temperature dependent. The snow unloading from the canopy, U_s , is defined as

$$U_s = I_s [f(T_c) + f(v)], \quad (6)$$

where $f(T_c)$ (s^{-1}) is the temperature-dependent unloading function, T_c (K) is the canopy air temperature, $f(v)$ (s^{-1}) is the wind-dependent unloading function, v ($m\ s^{-1}$) is the wind speed at the top of the canopy, and $f(T_c)$, is defined as

$$\begin{aligned} f(T_c) &= 0, & \text{for } T_c < T_m \\ f(T_c) &= \frac{T_c - T_m}{C_T}, & \text{for } T_c \geq T_m \end{aligned} \quad (7)$$

where T_m (K) is the minimum temperature above which snow unloading begins. The value is suggested as $T_m = 270.15\ K$ ($-3^\circ C$; Roesch et al., 2001) and is a tunable parameter in SUMMA (Table 3). C_T (K s), is an empirical constant for the temperature unloading function. This value is suggested as $C_T = 1.87 \times 10^5\ K\ s$ (Roesch et al., 2001) and is a tunable parameter in SUMMA (Table 3). Once $T_c \geq T_m$, snow unloads from the canopy onto the snowpack below at a rate, U_s , which increases with increasing T_c .

The wind-dependent unloading function, $f(v)$, is defined as

$$\begin{aligned} f(v) &= 0, & \text{for } v < v_m \\ f(v) &= \frac{v}{C_v}, & \text{for } v \geq v_m \end{aligned} \quad (8)$$

where C_v (m) is an empirical constant for wind unloading function, and v_m ($m\ s^{-1}$) is the minimum wind speed required for wind-dependent unloading to occur. Both C_v and v_m are tunable parameters in SUMMA (Table 3). Once $v \geq v_m$, intercepted snow unloads from the canopy at a rate, U_s , which increases with increasing v . Independent of the unloading parameterizations, snow in the canopy can melt as liquid water onto the snowpack below (see Section 3.2).

3.3. Model Evaluation Metrics

As described in Section 3.1, the canopy interception data set consists of a binary time series of snow absence or presence in the canopy. To evaluate the model performance, the model output was reduced to a binary data set, assuming that I_s less than $2\ kg\ m^{-2}$ was not a hydrologically significant interception event (Schmidt & Gluns, 1991), and only when simulated I_s was greater than $2\ kg\ m^{-2}$ was it deemed that snow was present in the canopy.

Table 4
Confusion Matrix Used to Describe the Performance of the Binary Unloading Model to the Binary Interception Observations

		Observations of snow in the canopy	
		Snow	No snow
Modeled snow in the canopy	Snow	True Positive (TP)	False Positive (FP)
	No snow	False Negative (FN)	True Negative (TN)

The binary time series were compared to determine the following metrics: True Positive (TP), when the model and the observations have snow in the canopy, False Positive (FP), when the model has snow in the canopy but the observations do not, True Negative (TN), when the model and the observations do not have snow in the canopy, and False Negative (FN), when the model does not have snow in the canopy, but the observations do (Table 4).

The binary evaluation metric, Balanced Accuracy (BA), was used in this work to measure model performance. The BA score is the average accuracy obtained for either class (Brodersen et al., 2010), defined as

$$BA = \frac{1}{2} \left(\frac{TP}{TP + FN} + \frac{TN}{TN + FP} \right). \quad (9)$$

The BA score is symmetric in its weight for both TP and TN results; thus, it captures when the model performs accurately in both the presence and absence of snow in the canopy. The *F*-score is another metric used to evaluate binary data, which excludes TN values (Olson & Delen, 2008). This has often been used to evaluate snow covered area products since the absence of TN values prevents unfairly weighing summer periods of no snow. We only evaluated interception during the winter months; thus, all components of the confusion matrix are important when evaluating model performance in this work (Table 4). The BA score can range from 0 to 1, where 0 would mean there are no time steps where the model and observations agree, and 1 means the model and observations agree at every time step, resulting in only TP and TN outcomes.

We determined that the model BA results were not sensitive to the resolution of the interception observations, for observations every 6 hr or shorter (Table S1 in Supporting Information S1). Thus, model performance was not impacted by comparing the model simulations with observational data sets of different temporal resolutions (e.g., hourly at Niwot Ridge and every 3 hr at other sites; Section S2.1 in Supporting Information S1). It is important to note that interception observations created from time-lapse photography are limited to daylight hours (e.g., only including daytime temperature ranges and wind patterns). This could bias the unloading parameterizations to only capture physical interception and unloading processes that occur during the day. However, the albedo in the canopy only matters during the day, thus this analysis works for our application.

3.4. Model Calibration

As shown in Section 3.2, each unloading parameterization has one or more tunable parameters. To answer our question about the influence of parameter calibration, we calibrated *k* from the Exponential-Decay unloading parameterization for *k* values up to $k = 2.0E-7 \text{ s}^{-1}$, which corresponds to 22 days *e*-folding time (Table 3). We evaluated all the parameters in the Wind-Temperature scheme and found *C_v* to be the most sensitive parameter (Section S2.3 in Supporting Information S1). To fairly compare models with the same degrees of freedom, we only varied *C_v* and kept all other parameters from the Wind-Temperature unloading scheme at their default values. Because the only tunable parameter in the Melt unloading parameterization, *r*, relates to the quantities of solid versus liquid snow leaving the canopy during melt, it is unrelated to timing and could not be calibrated using photographic data alone. Therefore, we left the value at the default, 0.4, throughout. Canopy melt rates are calculated physically within SUMMA and are not parameterized within the unloading schemes.

Model calibration was conducted by running model simulations for the entire water year compared against the entire water year of observational data with parameter values for all unloading schemes spanning five times the full suggested range (Table 3). The calibrated parameter values were selected by the simulations that produced the highest BA score for each site. Since our observations were limited to a single water year at each site, split

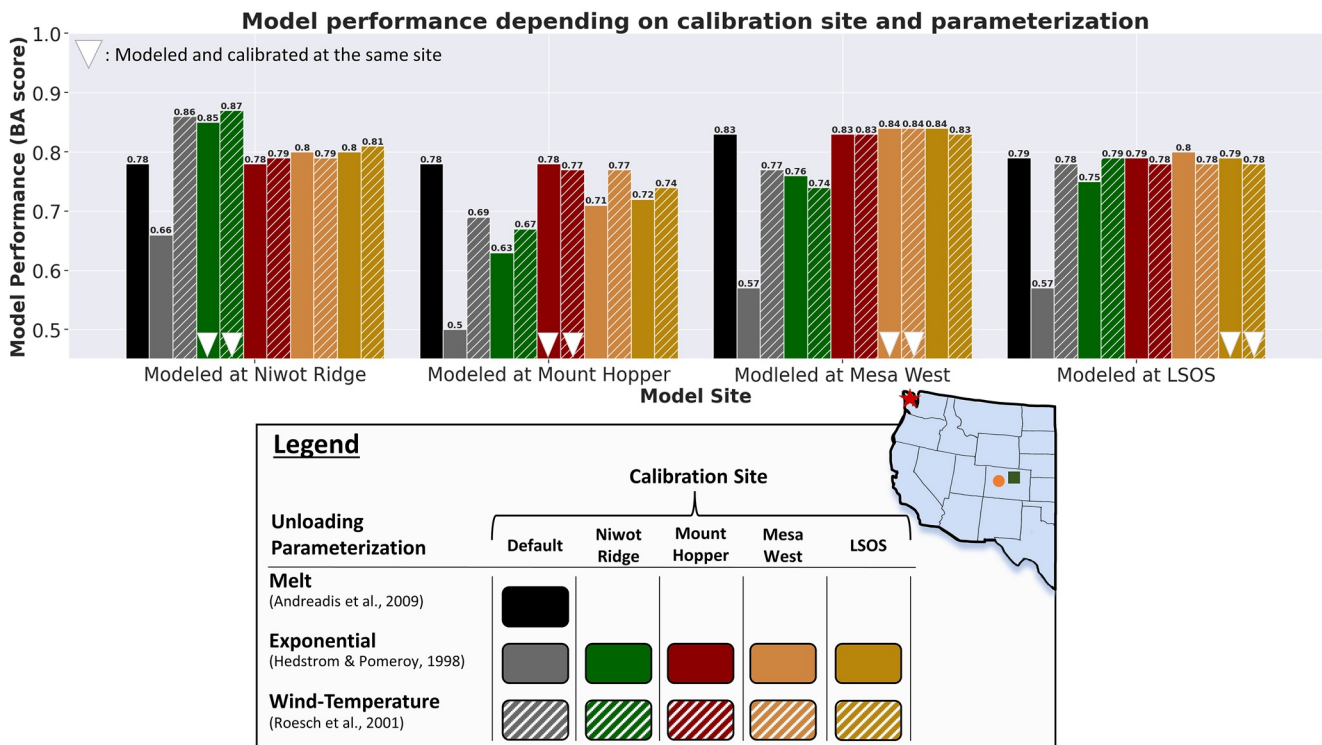


Figure 3. Model performance (Balanced Accuracy (BA) score) grouped by model site, dependent on calibration site and parameterization. Simulations calibrated at Niwot Ridge are in green, Mount Hopper in red, Mesa West in orange, and LSOS in yellow. Melt unloading is in black, Exponential-Decay unloading is in a solid color for each site's color, and Wind-Temperature unloading has hashes for each site's color. Simulations run with default parameter values are in gray. The white triangle signifies model simulations that were modeled and calibrated at the same site.

calibration-validation was not possible, but future work with observations over multiple years at one site would make it possible for calibrated parameters to be transferred to another point in time.

4. Results

4.1. Model Performance

4.1.1. Default Parameter Values

Default Melt unloading performed well and consistently between the sites, with an average BA score of 0.795 across all sites. Default Exponential-Decay unloading performed the worst of all model simulations at every site, with the highest BA score of 0.66 at Niwot Ridge and lowest of 0.50 at Mount Hopper. Default Wind-Temperature unloading performed similarly to Melt unloading, with an average BA score of 0.775 across all sites, performing best at Niwot Ridge (BA score 0.86) and worst at Mount Hopper (BA score 0.69; Figure 3; Table S2 in Supporting Information S1).

4.1.2. Parameter Values Calibrated Locally

Exponential-Decay unloading had the largest increase in model performance between default and calibrated BA scores where it increased on average by 20% after calibration at all sites. After calibration, Exponential-Decay and Wind-Temperature unloading performed similarly at all sites (i.e., within 1% of each other). The highest performance is at Niwot Ridge with a BA score of 0.87 from calibrated Wind-Temperature unloading. The difference between default and calibrated Wind-Temperature unloading performance was small (i.e., <1%) at Niwot Ridge and LSOS, but much larger (i.e., 8% increase in performance after calibration) at Mount Hopper and Mesa West (Figure 3; Table S2 in Supporting Information S1). Differences between in situ versus HRRR meteorological forcing at Niwot Ridge were also small, 2–3% for all schemes (Table S2 in Supporting Information S1).

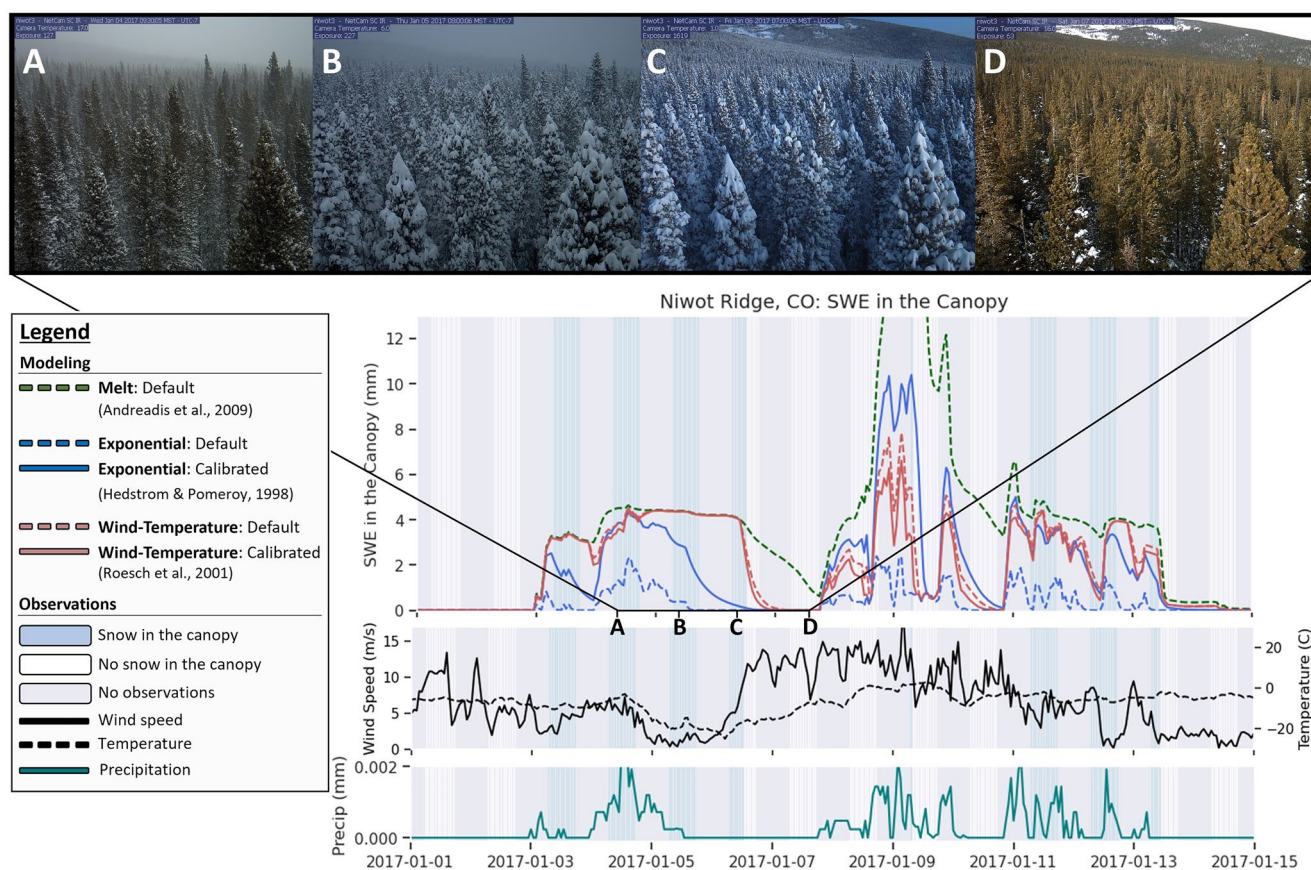


Figure 4. Case study 1: An interception event calibrated at Niwot Ridge, CO between 2 and 6 January 2017, when a large amount of snow accumulated in the canopy, shown in images a, b, and c, then snow unloaded from the canopy, shown in image d, a few hours later. Binary interception observations are represented by the same vertical shadings as in Figure 2b. The bottom plots show the corresponding wind speed (m s^{-1} ; solid black line on left axis), temperature ($^{\circ}\text{C}$; dashed black line on right axis), and precipitation (mm hr^{-1} ; solid teal line on bottom), for this time period.

4.1.3. Parameter Values Calibrated and Transferred to a Different Site

Both Exponential-Decay and Wind-Temperature simulations calibrated at Niwot Ridge did not transfer well to any of the other sites (i.e., 10–20% decrease in performance). Meanwhile models calibrated at Mount Hopper, Mesa West, and LSOS sites transferred well to each other. Melt unloading performed as well without calibration as any model calibrated at a different site, where only locally calibrated model setups exceeded it in performance. The exact BA scores for all combinations can be found in Figure 3 and in Table S2 in Supporting Information S1.

4.2. What Factors Lead to These Model Differences?

Since interception events occur on short time scales, it is difficult to visualize model simulations over the entire winter all at once. To better evaluate what is physically happening between the unloading parameterizations, we looked at three case studies. First, we examined an event at Niwot Ridge with both observed and simulated snow accumulation in the canopy while wind speeds were low (case study 1) and second, a storm with high wind speeds where no snow accumulated in the canopy, yet models simulated snow in the canopy (case study 2). The third case study is from Mount Hopper, WA where snow did not leave the canopy for >20 consecutive days, yet all three unloading parameterizations unloaded snow from the canopy (case study 3).

Case study 1 (Figure 4) highlights an interception event between 2 and 6 January when the mean wind speed during the storm was low (2.4 m s^{-1}) and observations showed a large accumulation of snow in the canopy at Niwot Ridge (Figures 4b and 4c). The parameterizations varied in the timing of snow unloading during this event. Melt unloading retained snow the longest, which resulted in 1 additional day of canopy-snow cover.

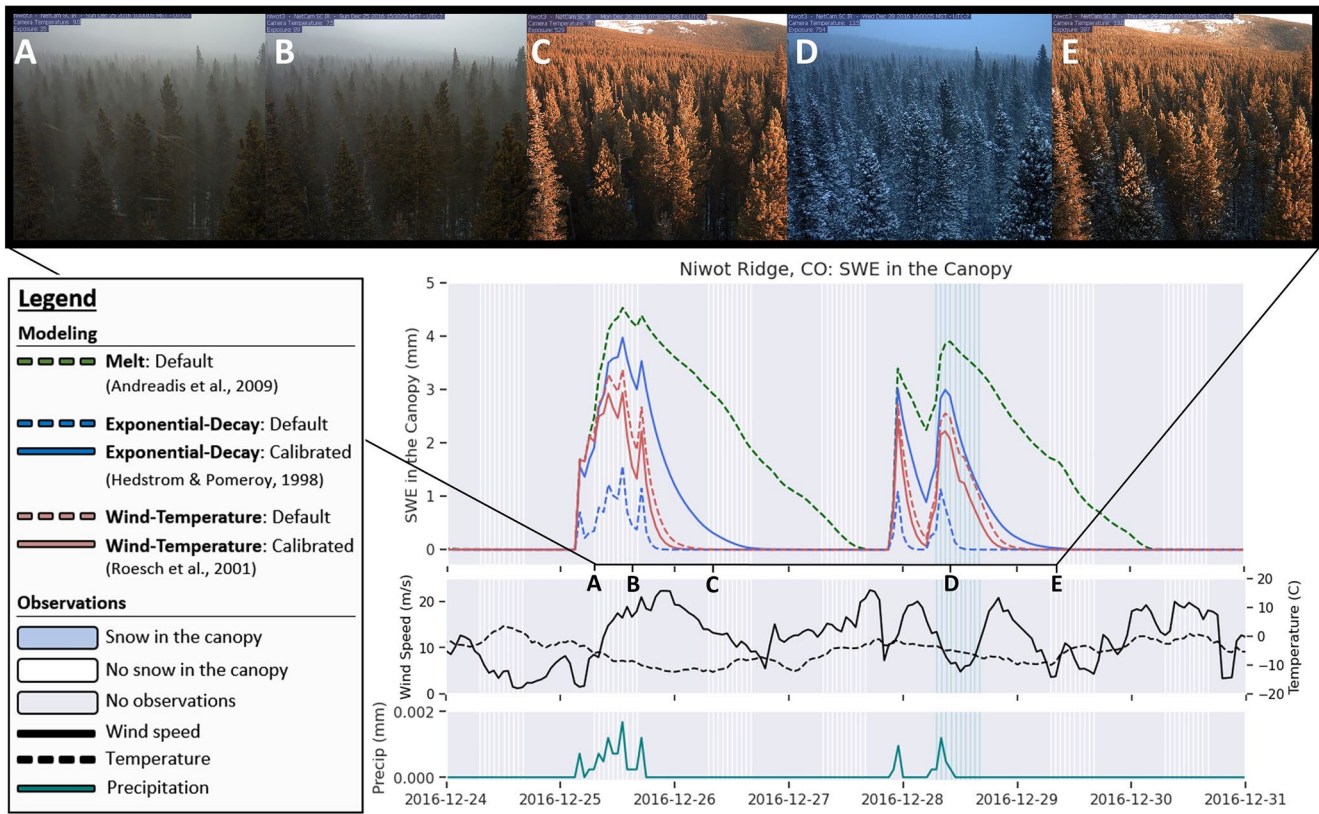


Figure 5. Case study 2: An interception event at Niwot Ridge, CO on 25 December 2016 when simulations modeled snow in the canopy during precipitation, but observations did not agree (shown in a, b, and c) and an interception event on 28 December where modeled simulations and observations both had snow in the canopy (shown in d), but Melt unloading modeled snow in the canopy for an extra day (shown in e). Binary interception observations are represented by the same vertical shadings as in Figure 2b. The bottom plots show the corresponding wind speed (m s^{-1} ; solid black line on left axis), temperature ($^{\circ}\text{C}$; dashed black line on right axis), and precipitation (mm hr^{-1} ; solid teal line on bottom), for this time period.

Calibrated Exponential-Decay, and default and calibrated Wind-Temperature all unloaded snow at the correct time on 6 January, yet they do so for different reasons. Wind-Temperature captured this unloading event by modeling the physical processes that contributed to snow leaving the canopy (i.e., an increase in wind speed to 13 m s^{-1} on 6 January; Figure 4) while calibrated Exponential-Decay provided a good estimate of the unloading event without additional physics included. However, when default parameter values were used, Exponential-Decay no longer provided a good estimate for the event, while default Wind-Temperature unloading still captured the event due to the physics in the parameterization.

Case study 2 (Figure 5) highlights two interception events, one on 25 December and one on 28 December. Time-lapse images from the first event on 25 December showed a precipitation event that occurred during high winds (i.e., averaging 17.9 m s^{-2}) and cold temperatures (i.e., averaging -3.4°C), which resulted in no snow accumulation in the canopy (Figures 5a–5c). Due to these conditions, snow remained in the canopy in Melt unloading simulations for two extra days compared to the other parameterizations. Default Exponential-Decay, and default and calibrated Wind-Temperature unloaded snow within 12 hrs of the event, where snow was unloaded throughout the event with Wind-Temperature simulations due to high wind speeds (Figure 5).

All three parameterizations accumulated snow in the canopy on 25 December, even though the observations showed no snow accumulation in the canopy. In SUMMA, canopy-snow interception and unloading are calculated simultaneously, thus snow can unload from the canopy as soon as snow is accumulated. Observations in case study 2 on 25 December (Figures 5a and 5b) show a situation where snow was blown out of the canopy before it could accumulate at all. The unloading schemes continuously unloaded snow from the canopy throughout this interception event, yet they still accumulated too much in the canopy.

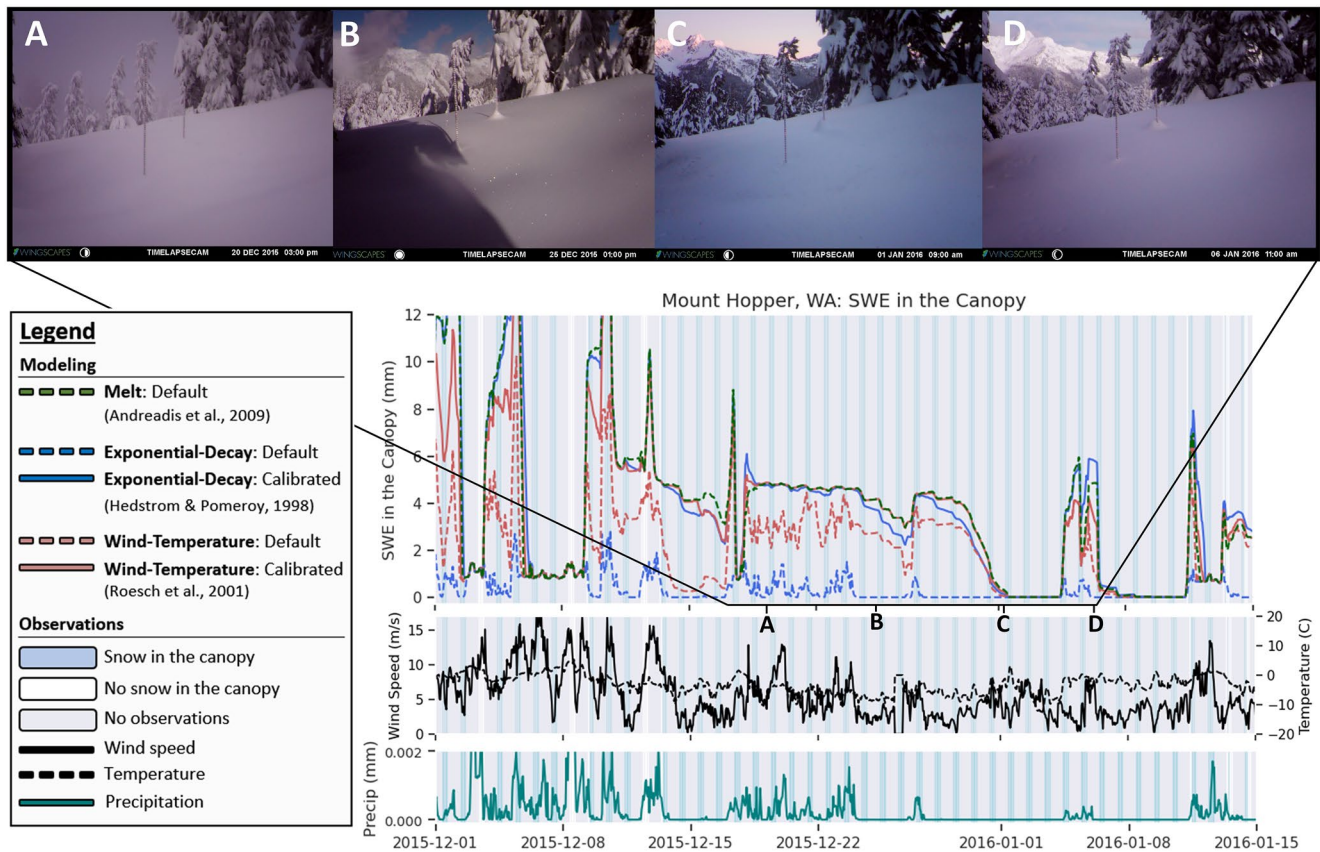


Figure 6. Case study 3: An interception event at Mount Hopper, WA between 15 December 2015 and 8 January 2016 when calibrated simulations modeled snow unloading from the canopy, but observations did not agree (shown in a, b, c, d). Binary interception observations are represented by the same vertical shadings as in Figure 2b. The bottom plots show the corresponding wind speed (m s^{-1} ; solid black line on left axis), temperature ($^{\circ}\text{C}$; dashed black line on right axis), and precipitation (mm hr^{-1} ; solid teal line on bottom), for this time period.

Observations from the second event highlighted on 28 December showed snow in the canopy (Figures 5d and 5e) while the wind speeds were low (i.e., average 6.1 m s^{-2}). During the night, the wind speed increased significantly to 20.4 m s^{-2} , and by morning all the snow unloaded from the canopy (Figure 5e). While the default and calibrated Exponential-Decay and Wind-Temperature simulations captured the timing of this unloading event, Melt unloading kept snow in the canopy for an extra day due to low temperatures.

Case study 3 (Figure 6) highlights 1.5 months at Mount Hopper, WA, where observations showed snow did not leave the canopy for over a month. During this month-long event, there was a high relative humidity (i.e., between 96% and 100%) with air temperatures hovering near freezing (i.e., between a low of -4.2 and high of 2.6°C). It is likely that snow became firmly attached to the canopy through melt-freeze cycles and near-constant precipitation (i.e., not purely rime formation), which resulted in a month-long canopy interception event (Figures 6a–6d). While snow remained in the canopy throughout the month, the viewer can observe that between images B and C there is an obvious decrease in the amount of snow in the canopy. This is a limitation of the binary interception observations since they only provide information on the presence or absence of snow, and not the amount (i.e., only capturing full, not partial, unloading events).

Before calibration, Exponential-Decay unloaded all the snow continuously throughout the month and improved after calibration to retain snow in the canopy longer. Wind-Temperature unloading performed similarly before and after local calibration, and default Melt unloading modeled this event similarly to the other two calibrated parameterizations (Figure 6).

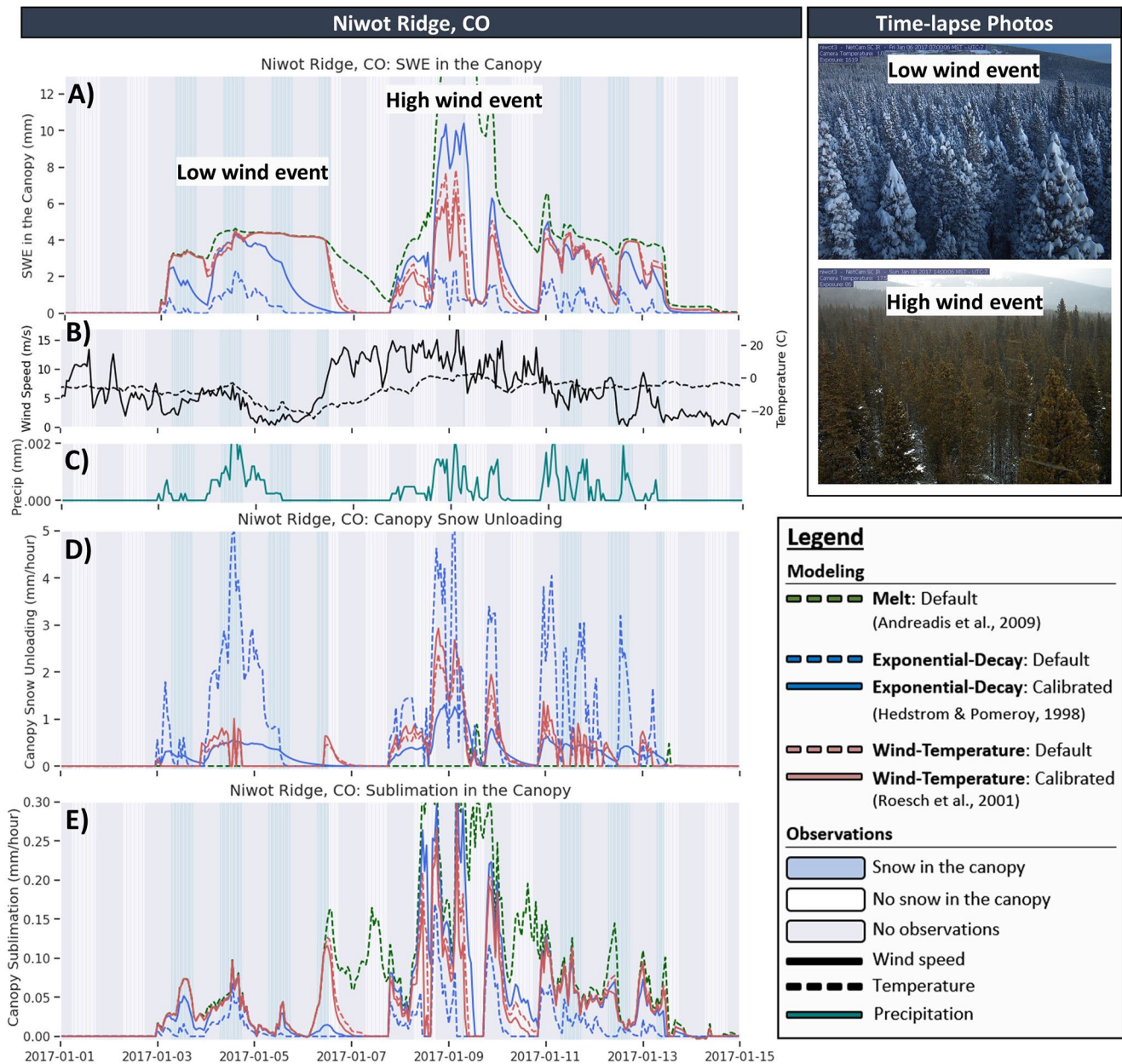


Figure 7. (a) SWE in the canopy (mm), (b) wind speed (m s^{-1} ; solid black line on left axis), and temperature ($^{\circ}\text{C}$; dashed black line on right axis), (c) precipitation (mm hr^{-1} ; solid teal line), (d) snow unloading from the canopy (mm hr^{-1}) representing only the snow unloaded from the canopy to the underlying snowpack, and (e) canopy sublimation (mm hr^{-1}) represented as a net loss from the hydrologic system (i.e., mm hr^{-1} of SWE) for Niwot Ridge, CO between 1 and 15 January 2017, highlighting a low wind event when snow remained in the trees and a high wind event when observations did not show snow in the canopy for default and locally calibrated simulations. Binary interception observations are represented by the same vertical shadings as in Figure 2b.

4.3. How Does Our Choice of Unloading Scheme Impact the Modeled Fate of Snow in the Canopy?

Case study 1 (Figure 4), from Section 4.2, was evaluated to determine how the canopy-snow unloading schemes influenced the snow lost from the canopy-snow sublimation (Figure 7).

Canopy-snow unloading (Figure 7d) and canopy sublimation (Figure 7e) were analyzed for the same period as case study 1 at Niwot Ridge. Default Exponential-Decay unloaded the most snow from the canopy, which resulted in the least canopy sublimation between all the parameterizations (Figures 7d and 7e). Canopy-snow unloaded from Wind-Temperature increased with increased windspeed, but since snow was unloaded during high wind events, there was less snow left to sublimate. For this case study, the large amount of snow in the canopy

Table 5

The Cumulative Sublimation of SWE in the Canopy (mm) and the Total Canopy Sublimation as a Percent of the Total Precipitation (%) for Each Unloading Parameterization

Unloading scheme	Melt		Exponential-Decay				Wind-Temperature			
	Total canopy sub. (mm)	% of total precip	Total canopy sub. (mm)		% of total precipitation		Total canopy sub. (mm)		% of total precipitation	
Calculation					Default (%)	Calibrated (%)			Default (%)	Calibrated (%)
Calibration	Default	Default (%)	Default	Calibrated			Default	Calibrated		
Niwot, CO (HRRR)	189.7	14.4	15.5	75.8	1.2	5.7	79.2	67.5	6.0	5.1
Mount Hopper, WA	42.9	2.9	4.0	41.8	0.3	2.9	26.7	40.7	1.8	2.8
Mesa West, CO	106.1	6.1	6.3	54.3	0.4	3.1	31.6	78.4	1.8	4.5
LSOS, CO	108.8	4.5	10.8	64.6	0.4	2.7	74.3	88.4	3.1	3.7

in the Melt parameterization unloaded the least amount of snow because the air temperature did not exceed 0°C (Figure 7b). Thus, Melt unloading had the most canopy sublimation between all the schemes (Figure 7e). Since sublimation rates increase with wind speed, keeping snow in the canopy during high wind speeds had a large impact of the fate of the snow in the canopy.

In addition to the unloading and sublimation rates from case study 1, cumulative canopy sublimation (Table 5), cumulative snow unloading and SWE on the ground (Table 6) were calculated for all four sites. The cumulative sublimation, snow unloading, snow throughfall, and SWE on the ground were further explored at the two sites where they were the most dissimilar, Niwot Ridge, CO for WY 2017 and Mount Hopper, WA for WY 2016 (Figure 8).

At Niwot Ridge, Melt unloaded the least amount of snow from the canopy with a total of 31.1 mm (Table 6; Figure 8b). Since snow remained in the canopy the longest, Melt unloading resulted in the largest net loss through canopy sublimation, with a cumulative loss of 189 mm of SWE in the canopy, which is 14.4% of total precipitation for that time period, compared to 2–6% on average for other simulations (Table 5; Figure 8b). While observations of sublimation, and specifically of canopy sublimation, are rare, Molotch et al. (2007) measured a cumulative canopy sublimation of 23.7 mm (i.e., 1.5% of precipitation) at Niwot Ridge, CO during WY 2002. Other studies at Niwot Ridge reported net sublimation from the snow surface of 15% of maximum snow accumulation (Hood et al., 1999).

At Niwot Ridge, default Melt and default Exponential-Decay resulted in a 19% difference in SWE on the ground below the canopy between the schemes, which is largely attributed to the large difference in canopy sublimation (Figure 8d; Tables 5 and 6). The remaining differences in SWE under the canopy were due to increased snow throughfall within the canopy when the Melt unloading scheme reached the maximum interception capacity (Figure 8c).

Table 6

The Cumulative Snow Unloading From the Canopy (mm) as a Direct Result of the Snow Unloading Parameterizations and Snow Totals (mm) for Each Site

Unloading scheme	Melt		Exponential-Decay				Wind-Temperature				
	Snow unload (mm)	Total snow (mm)	Snow unload (mm)		Total snow under canopy (mm)		Snow unload (mm)		Total snow under canopy (mm)		Total snowfall (mm)
Calculation											
Calibration	Default	Default	Default	Calibrated	Default	Calibrated	Default	Calibrated	Default	Calibrated	
Niwot, CO (HRRR)	31.1	1,093	1,054	432	1,325	1,236	371	434	1,221	1,246	1,319
Mount Hopper, WA	119	1,418	1,299	40.1	1,606	1,297	606	175	1,484	1,396	1,455
Mesa West, CO	15.4	1,628	1,750	199	1,691	1,716	397	138	1,716	1,662	1,730
LSOS, CO	38.4	2,376	1,604	226	2,492	2,426	394	230	2,412	2,394	2,403

Note. Not including loss of snow in the canopy from latent heat fluxes, such as evaporation and sublimation.

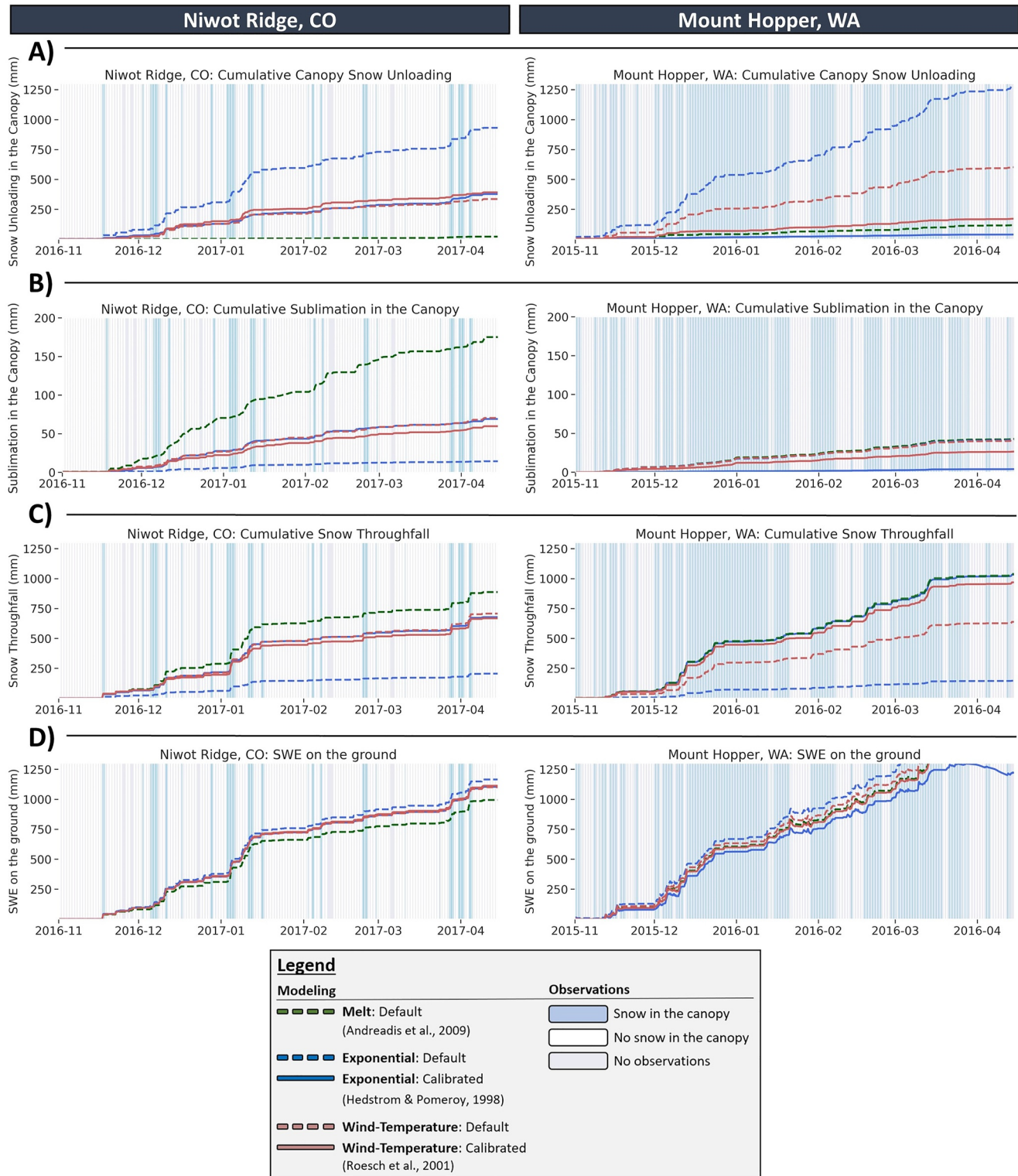


Figure 8. (a) Cumulative snow unloading from the canopy (mm), (b) cumulative sublimation of SWE in the canopy (mm), (c) cumulative snow throughfall (mm), and (d) cumulative SWE on the ground under the canopy (mm) for Niwot Ridge, CO (left) and Mount Hopper, WA (right) for default and locally calibrated simulations. Binary interception observations are represented by the same vertical shadings as in Figure 2b.

At Mount Hopper, there were comparably small amounts of sublimation in the canopy. Instead the net loss of SWE in the canopy at Mount Hopper was driven by canopy-snow unloading for all the simulations, where default Exponential-Decay unloading had a cumulative 1,054 mm of canopy-snow unloaded (Figure 8a; Table 6); This resulted in a 12% difference in SWE on the ground between Melt and default Exponential-Decay at Mount Hopper, and a 21% difference in SWE on the ground between default and calibrated Exponential-Decay unloading (Figure 8d; Table 6).

Melt unloading consistently resulted in the smallest cumulative snow unloading (Table 6) and largest cumulative canopy sublimation (Table 5) for all four sites. Default Exponential-Decay simulations consistently resulted in the largest cumulative snow unloading (Table 6) and the least cumulative canopy sublimation (Table 5) for all four sites.

5. Discussion

5.1. Canopy Albedo Implications of the Different Canopy-Snow Unloading Parameterizations

A large source of error in global climate models is the snow albedo feedback over forested regions during the winter (Thackeray et al., 2014). To understand the snow albedo feedback under different climate change scenarios, we need models that simulate snow interception and associated canopy land surface albedo correctly. Thus, we estimate one component of the snow albedo feedback, the canopy albedo, for the three unloading schemes over the winter season.

SUMMA does not explicitly use snow in the canopy in calculations of radiative transfer, meaning we cannot use SUMMA's simulated energy balance in the canopy to quantify the effect of the different unloading schemes on the canopy albedo. Therefore, we used SUMMA's modeled snow presence and absence to determine times with snow in the canopy, and combined that with published albedo values, to determine the reflected radiation at each time step. We used the summer albedo for conifers from Betts and Ball (1997), 0.083, as reported in Roesch et al. (2001) for times with no snow in the canopy, and 0.283, a 20% increase, for times with snow in the canopy. The increase was chosen as a conservative estimate based on observations from Roesch et al. (2001), who reported an increase of about 20% in albedo with snow in the canopy for the boreal forest, and Webster and Jonas (2018), who found that canopy albedo increased by about 30% with interception compared to no interception in the Eastern Swiss Alps.

The influence of a 20% increase in canopy albedo would be larger on days with more incoming solar radiation. Therefore, we combined the incoming solar radiation with the respective canopy albedo values above for snow-off and snow-on canopy conditions in Equation 10 to determine the approximate average reflected radiation over the season for each model situation in $W m^{-2}$ as

$$SW_{\text{reflected}} = SW_{\text{in}} \alpha, \quad \text{where } \alpha_{\text{snowOff}} = 0.083 \quad (10)$$

$$\alpha_{\text{snowOn}} = 0.083 + 0.20 = 0.283$$

where SW_{in} ($W m^{-2}$) is the incoming solar radiation, α , is the canopy albedo depending on the binary presence or absence of snow in the canopy. This calculation was done hourly from 1 December to 1 April for all sites and model simulations, from which we calculated the average reflected shortwave, $SW_{\text{reflected}}$ ($W m^{-2}$; Figure 9).

The total number of days snow is in the canopy between 1 December and 1 April was calculated from hourly model simulations (Figure 9a). Since the time-lapse observations are not continuous like the hourly model simulations, we interpolated between observations to fill missing data for this estimate. If there was snow in an observation, but no snow in the next observation, the time period between the two was split in half, snow and no snow, during the missing time steps. This interpolation was only done to provide an observational comparison to the model simulation reflected radiation estimates in Figure 9. During the actual model evaluation, simulations were only evaluated at time steps when there are physical observations (Section 3.3).

Melt unloading simulations consistently produced the most canopy-snow covered days at every site (Figure 9a), which resulted in the highest estimated average winter canopy albedo (Figure 9c). Default Exponential-Decay unloading produced the least canopy-snow covered days and the lowest average winter canopy albedo across all the sites. Mesa West had the largest variability in average reflected shortwave and average canopy albedo between

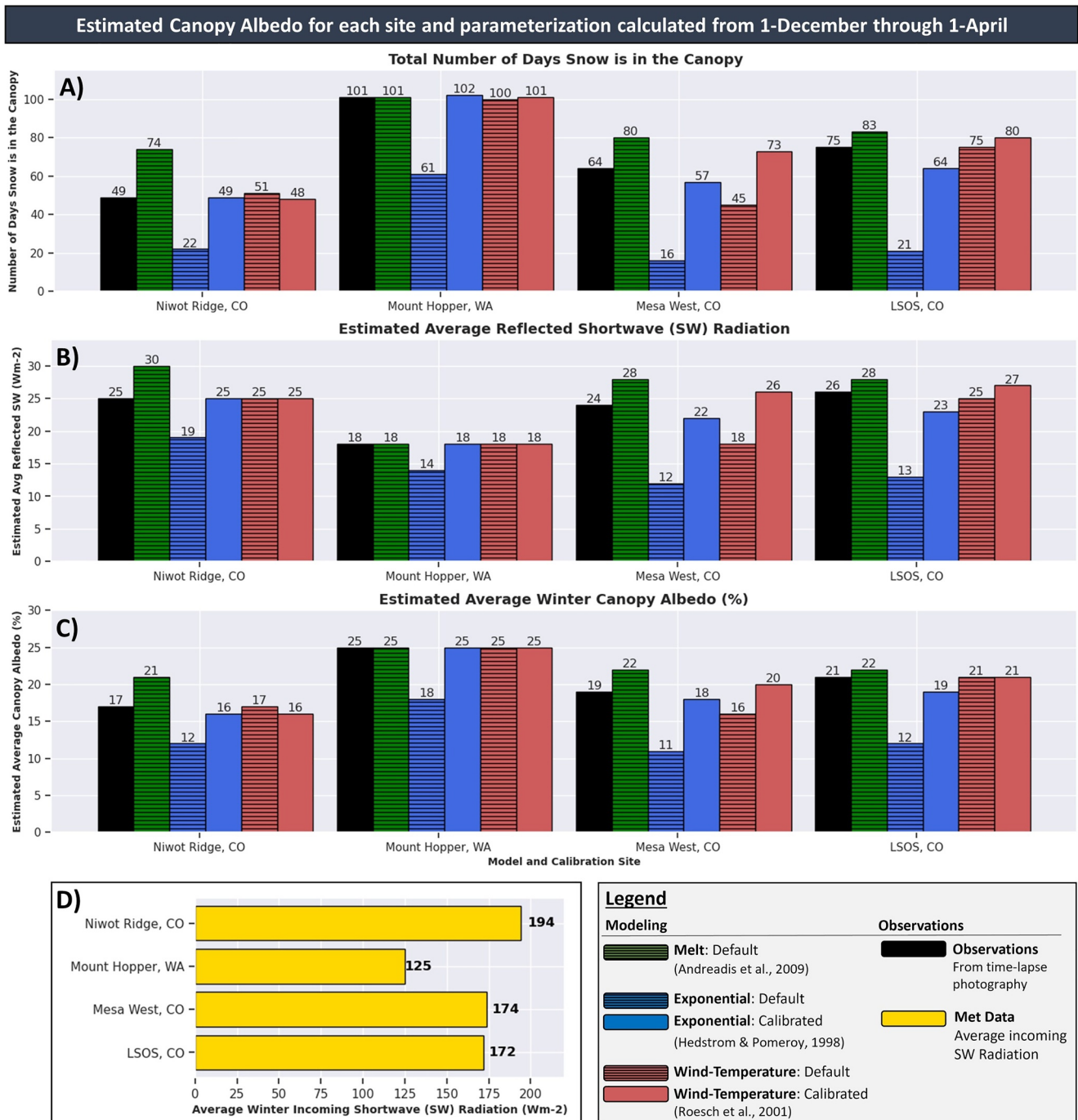


Figure 9. For the period between 1 December and 1 April, (a) the total number of days that snow is observed and modeled in the canopy, (b) estimated average reflected shortwave (SW) radiation ($W m^{-2}$), (c) estimated average canopy albedo, %, calculated for each site and parameterization, and (d) average incoming shortwave radiation ($W m^{-2}$). Observations from time-lapse photography are in black, average winter incoming shortwave radiation is in yellow, calculated over day and night, Melt unloading in green, default Exponential-Decay in blue stripes with calibrated in solid blue, and default Wind-Temperature in red stripes with calibrated in solid red.

the unloading parameterizations. There is up to a 10% difference in average canopy albedo and $10 W m^{-2}$ difference in average reflected shortwave radiation as a function of the unloading scheme for 1 December through 1 April (Figure 9).

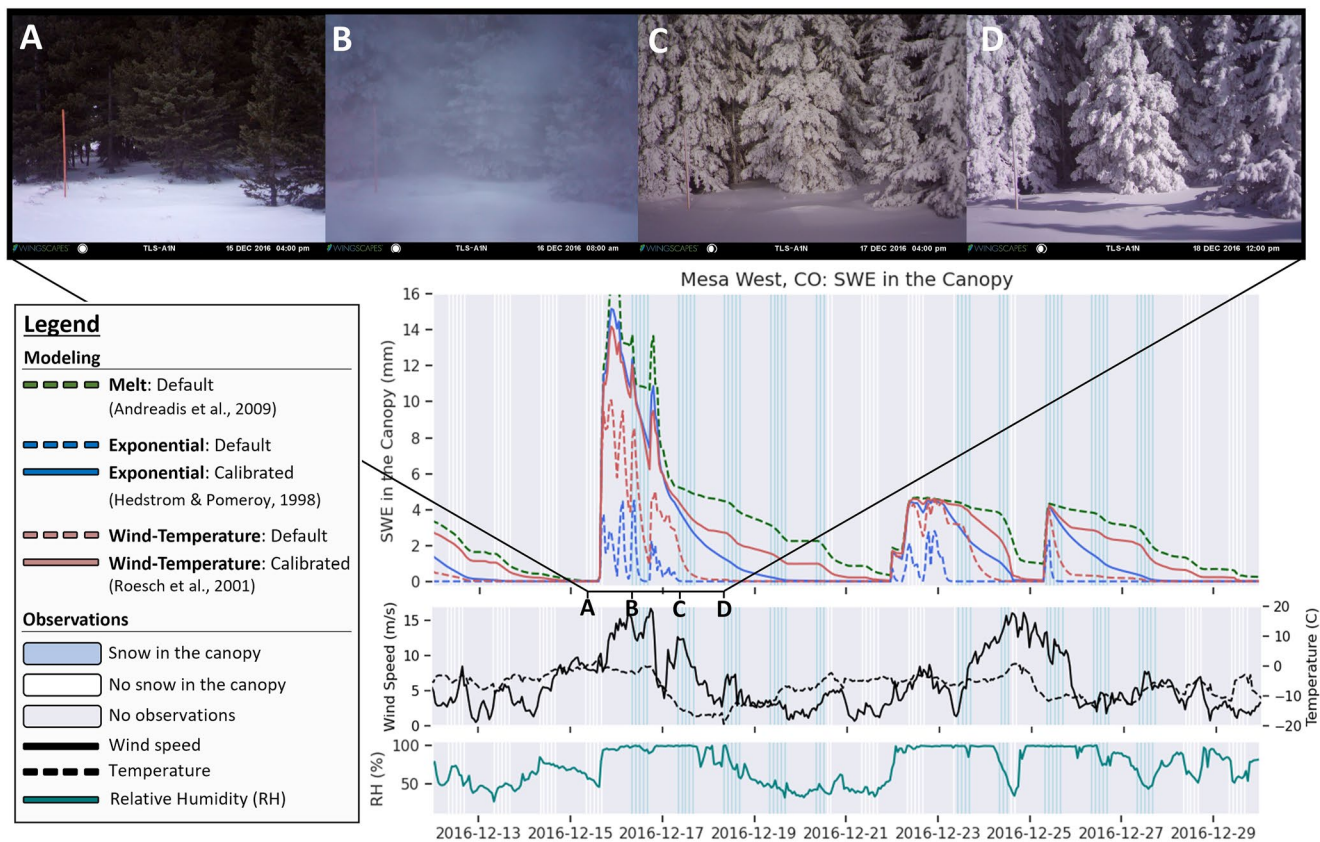


Figure 10. Case study 4: An interception event at Mesa West (MW), Grand Mesa, CO between 16 and 21 December 2016 when calibrated simulations unloaded snow from the canopy 1 day after precipitation (shown in b), but observations show snow persisted in the canopy for many days (shown in c and d). Binary interception observations are represented by the same vertical shadings as in Figure 2b. The bottom plots show the corresponding wind speed (m s^{-1} ; solid black line on left axis), temperature ($^{\circ}\text{C}$; dashed black line on right axis), and relative humidity (RH, %; solid teal line on bottom) for this time period.

For context, the change in industrial-era radiative forcing by CO_2 is $+1.82 \text{ W m}^{-2}$ and that from all greenhouse gases is $+2.83 \text{ W m}^{-2}$ (Myhre et al., 2013), which is less than a third of the spread in reflected radiation found between these unloading parameterizations (i.e., $+10 \text{ W m}^{-2}$). These results are comparable to variations in snow albedo caused by light-absorbing particles on snow (Skiles et al., 2018) and similar to the spread found among numerous climate models by Thackeray et al. (2014). The spread in albedo in Thackeray's simulations was 12%, which led to a 4°C change in the simulated seasonal mean near-surface air temperature over the midhigh latitudes, which is almost as large as the total CMIP5 ensemble's intermodal spread of 5°C (Thackeray et al., 2014). Our results support their conclusion that many climate model errors can be tracked back to features in canopy-snow parameterizations used in land surface models (Thackeray et al., 2014).

5.2. Physical Processes Missing From the Canopy-Snow Unloading Parameterizations

The calibrated snow unloading coefficients in the Exponential-Decay unloading scheme resulted in slower unloading rates at Mount Hopper and Mesa West compared to Niwot Ridge (Table 3). One reason snow stayed in the canopy longer at these locations was due to the presence of rime, observed in the photographs. This is illustrated with in case study 4 from Mesa West on Grand Mesa, where rime accumulation in the canopy persisted far past the modeled canopy snow (Figure 10). Both the default Exponential-Decay and Wind-Temperature models simulated snow being removed from the canopy too quickly compared to observations (Figure 10).

Rime ice forms when supercooled water droplets in clouds are carried by strong winds to engulf terrain (Whiteman & Garibotti, 2013). Rime formation often occurs with high wind velocities, high humidities, and air temperatures between -2 and -8°C (Whiteman & Garibotti, 2013). Photographs from 16 December 2016 (Figure 10b) showed that the trees at Mesa West became immersed in a fog of supercooled liquid droplets. The supercooled fog

droplets were deposited onto the canopy surface, where they froze (Figure 10c) and remained in the canopy for 5 consecutive days. The meteorological conditions on 16 December closely matched ideal rime formation conditions with an average wind speed of 14.6 m s^{-1} , average relative humidity of 98%, and average air temperature of -4.7°C on that day (Figure 10b).

Due to the high winds of $10\text{--}15 \text{ m s}^{-1}$ during the interception event, the default Wind-Temperature scheme unloaded all snow from the canopy within 2 days. Melt and calibrated Wind-Temperature unloading both kept snow in the canopy during the entire interception event for different reasons. Rime was well-attached to the tree and not easily removed by wind; instead, only melting could remove it. This melting worked in the Melt and Wind-Temperature schemes on 24 December 2016 when the temperature was above 0°C —likely driven by solar radiation. The calibrated Wind-Temperature unloading scheme by design matched the most common unloading pattern during the season, and since rime appeared frequently at this location, the calibrated scheme became less sensitive to high winds.

SUMMA models frost deposition in the canopy when the latent heat flux associated with moisture transfer from the canopy to the canopy air space is greater than 0 W m^{-2} . While this modeled frost is not currently used in interception or unloading of canopy-snow in SUMMA, the timing of the calculated frost conditions could be used to inform unloading parameterizations of rime conditions. Additional time-lapse photography, classified by citizen scientists, could be used to capture riming events more accurately. This would require photographs to be taken on the windward side of trees from just a few meters away to view the physical structure of the snow accumulating on the canopy (e.g., a snowpack accumulating on top of the branches versus rime ice forming on the top and bottom of the branches). This type of riming interception data set could be used to evaluate the timing of existing modeled rime in SUMMA and once validated, used to inform, and improve canopy-snow unloading parameterizations.

It is important to note that it is likely not pure rime that accumulated during events like this, but instead deposits from a mixture of snow, fog, rimed snowflakes, graupel, and even rain that coated the canopy (Makkonen, 2000; Whiteman & Garibotti, 2013). Therefore, an updated unloading scheme may have to account for this mixture of complex physical processes to correctly capture riming in the canopy.

6. Conclusions

Time-lapse photography was a great tool to get information about snow conditions in remote environments during winter. Thousands of citizen science volunteers were able to process time-lapse photography of interception quickly and accurately, making citizen science platforms, such as Zooniverse, a great contribution to science by producing novel data sets that involve thousands of volunteers. The novel interception data set produced from this work was used to evaluate three snow unloading parameterizations in SUMMA (Table 1).

Wind-Temperature unloading performed well without calibration across sites, specifically in cold climates, such as Niwot Ridge, where wind is the dominant unloading factor and rime accretion is low. At sites where air temperature and relative humidity are frequently favorable to riming, Wind-Temperature unloading should be locally calibrated to account for longer interception events with less sensitivity to wind, otherwise Melt unloading can be used without calibration. The absence of model physics in Exponential-Decay unloading required the rate of unloading to be calibrated locally, and it can only be transferred to sites with similar unloading patterns.

Mesa West had the largest variability in the average reflected shortwave and average canopy albedo between the parametrizations (i.e., 10% difference in average albedo and 10 W m^{-2} difference in reflected shortwave on average over days and nights from 1 December to 1 April), due to the existing models' inability to capture rime related interception events. Our results support Thackeray et al.'s (2014) conclusion that many climate model errors can be traced back to features in canopy-snow parameterizations used in land surface models.

The evaluation of canopy-snow unloading parametrizations could be improved with time-lapse images that span multiple years for each site to determine the transferability of calibrated schemes in 1 year to another point in time at the same site. While Wind-Temperature unloading comes close, for an unloading parameterization to transfer across all climates without any calibration, it must include model physics associated with rime conditions.

In summary, the choice of canopy-snow unloading scheme impacted the partitioning of water storage between snow on the ground and snow lost to canopy sublimation. It also resulted in differences in the canopy albedo feedback to the atmosphere. Due to lack of observations (Lundquist et al., 2021), these processes are often overlooked in hydrology. Remote time-lapse cameras and citizen science provide one path for new observations and new understanding.

Data Availability Statement

The data generated from the citizen science platform, Zooniverse, would not be possible without the Snow Spotter founder, Max Mozer, and the nearly 8,000 individual citizen science volunteers. We are deeply grateful for the thousands of collective hours all the citizen scientists put into generating this data product. Additionally, data used in this research includes 2017 NASA SnowEx time-lapse photography, PhenoCam Network time-lapse photography, and OLYMPEx time-lapse photography. We would like to thank all the participants from these data missions for their time and are deeply grateful for the availability of these images. This publication uses data generated via the [Zooniverse.org](https://www.zooniverse.org) platform, development of which is funded by generous support, including a Global Impact Award from Google, and by a grant from the Alfred P. Sloan Foundation. Funding for AmeriFlux data resources was provided by the U.S. Department of Energy's Office of Science. The python analysis and notebooks to recreate model simulations and figures are provided in a GitHub repository (https://github.com/cassielumbrazo/summa_snow_unloading_analysis). The final Zooniverse canopy-snow interception data set is published on Zenodo (Lumbrazo et al., 2022; <https://doi.org/10.5281/zenodo.5918637>).

Acknowledgments

We gratefully acknowledge funding support from the Steve and Sylvia Burges Endowed Presidential Fellowship in Civil and Environmental Engineering and the NSF Award CBET-1703663, Managing Forests for Snow, Water, and Sustainable Ecosystems. We gratefully acknowledge computational resources from Pangeo, the Computational Hydrology Research Group, and the Mountain Hydrology Research Group at the University of Washington. We would like to acknowledge the effort of the Editor, Kamini Singha, the Associate Editor, Nick Rutter, and the three anonymous reviewers for their comments that improved the quality of this manuscript.

References

- Andreadis, K. M., Storck, P., & Lettenmaier, D. P. (2009). Modeling snow accumulation and ablation processes in forested environments. *Water Resources Research*, 45, W05429. <https://doi.org/10.1029/2008WR007042>
- Bartlett, P. A., & Verseghy, D. L. (2015). Modified treatment of intercepted snow improves the simulated forest albedo in the Canadian Land Surface Scheme. *Hydrological Processes*, 29(14), 3208–3226. <https://doi.org/10.1002/hyp.10431>
- Betts, A. K., & Ball, J. H. (1997). Albedo over the boreal forest. *Journal of Geophysical Research*, 102(96), 901–909. <https://doi.org/10.1029/96JD03876>
- Bonan, G. B., Pollard, D., & Thompson, S. L. (1992). Effects of boreal forest on global climate. *Nature*, 359, 716–718. <https://doi.org/10.1038/359716a0>
- Brodersen, K. H., Ong, C. S., Stephan, K. E., & Buhmann, J. M. (2010). The balanced accuracy and its posterior distribution. *Proceedings-International Conference on Pattern Recognition*, 3121–3124. <https://doi.org/10.1109/ICPR.2010.764>
- Clark, M. P., Nijssen, B., Lundquist, J., Kavetski, D., Rupp, D., Woods, R., et al. (2015a). A unified approach to process-based hydrologic modeling. Part 1: Modeling concept. *Water Resources Research*, 51, 2498–2514. <https://doi.org/10.1002/2015WR017198>
- Clark, M. P., Nijssen, B., Lundquist, J., Kavetski, D., Rupp, D., Woods, R., et al. (2015b). A unified approach for process-based hydrologic modeling: Part 2. Model implementation and example applications. *Water Resources Research*, 51, 2515–2542. <https://doi.org/10.1002/2015WR017200>
- Clark, M. P., Nijssen, B., Lundquist, J., Kavetski, D., Rupp, D., Woods, R., et al. (2015c). *The structure for unifying multiple modeling alternatives (SUMMA), version 1: Technical description*, NCAR Technical Note NCAR/TN-514+STR (p. 54). National Center for Atmospheric Research. <https://doi.org/10.5065/D6WQ01TD>
- Clark, M., Wood, A., Nijssen, B., Bennett, A., Knoben, W., & Lumbrazo, C. (2020). SUMMA v3.0.3 [Dataset]. Zenodo. <https://doi.org/10.5281/zenodo.4558054>
- Currier, W. R., Pflug, J., Mazzotti, G., Jonas, T., Deems, J. S., Bormann, K. J., et al. (2019). Comparing aerial lidar observations with terrestrial lidar and snow-probe transects from NASA's 2017 SnowEx campaign. *Water Resources Research*, 55, 6285–6294. <https://doi.org/10.1029/2018WR024533>
- Currier, W. R., Thorson, T., & Lundquist, J. D. (2017). Independent evaluation of frozen precipitation from WRF and PRISM in the Olympic mountains. *Journal of Hydrometeorology*, 18(10), 2681–2703. <https://doi.org/10.1175/jhm-d-17-0026.1>
- Essery, R. (1998). Boreal forests and snow in climate models. *Hydrological Processes*, 12(10–11), 1561–1567. [https://doi.org/10.1002/\(SICI\)1099-1085\(199808/09\)12:10<1561::AID-HYP681>3.0.CO;2-B](https://doi.org/10.1002/(SICI)1099-1085(199808/09)12:10<1561::AID-HYP681>3.0.CO;2-B)
- Essery, R. L. H., Best, M. J., Betts, R. A., Cox, P. M., & Taylor, C. M. (2003). Explicit representation of subgrid heterogeneity in a GCM land surface scheme. *Journal of Hydrometeorology*, 4(3), 530–543. [https://doi.org/10.1175/1525-7541\(2003\)004<0530:EROSHI>2.0.CO;2](https://doi.org/10.1175/1525-7541(2003)004<0530:EROSHI>2.0.CO;2)
- Gelfan, A. N., Pomeroy, J. W., & Kuchment, L. S. (2004). Modeling forest cover influences on snow accumulation, sublimation, and melt. *Journal of Hydrometeorology*, 5, 785–803. [https://doi.org/10.1175/1525-7541\(2004\)005<0785:MFCIOS>2.0.CO;2](https://doi.org/10.1175/1525-7541(2004)005<0785:MFCIOS>2.0.CO;2)
- Hedstrom, N. R., & Pomeroy, J. W. (1998). Measurements and modelling of snow interception in the boreal forest. *Hydrological Processes*, 12, 1611–1625. [https://doi.org/10.1002/\(SICI\)1099-1085\(199808/09\)12:10<1611::AID-HYP684>3.0.CO;2-4](https://doi.org/10.1002/(SICI)1099-1085(199808/09)12:10<1611::AID-HYP684>3.0.CO;2-4)
- Hood, E., Williams, M., & Cline, D. (1999). Sublimation from a seasonal snowpack at a continental, mid-latitude alpine site. *13(12–13)*, 1781–1797. [https://doi.org/10.1002/\(SICI\)1099-1085\(199909\)13:12<1781::AID-HYP860>3.0.CO;2-C](https://doi.org/10.1002/(SICI)1099-1085(199909)13:12<1781::AID-HYP860>3.0.CO;2-C)
- Horel, J., & Blaylock, B. (2019). *Archive of the high resolution rapid refresh mode*. University of Utah Center for High Performance Computing. <https://doi.org/10.7278/S5JQ0Z5B>
- Houze, R. A., McMurdie, L. A., Petersen, W. A., Schwall Er, M. R., Baccus, W., Lundquist, J. D., et al. (2017). The Olympic mountains experiment (Olympex). *Bulletin of the American Meteorological Society*, 98(10), 2167–2188. <https://doi.org/10.1175/BAMS-D-16-0182.1>
- Kim, E., Gatebe, C., Hall, D., Misakonis, A., Elder, K., Marshall, H. P., et al. (2017). Nasa's SnowEx campaign: Observing seasonal snow in a forested environment NASA Goddard Space Flight Center, 2 USRA, 3 aerospace corp., 4 ATA aerospace, 5 US forest service. *IEEE Transactions on Geoscience and Remote Sensing*, 1388–1390.

- Klein, A. G., Hall, D. K., & Riggs, G. A. (1998). Improving snow cover mapping in forests through the use of a canopy reflectance model. *Hydrological Processes*, *12*, 1723–1744. [https://doi.org/10.1002/\(SICI\)1099-1085\(199808/09\)12:10<1723::AID-HYP691>3.0.CO;2-2](https://doi.org/10.1002/(SICI)1099-1085(199808/09)12:10<1723::AID-HYP691>3.0.CO;2-2)
- Lumbrazo, C., Mozer, M., Currier, W. R., & Lundquist, J. (2022). Snow spotter canopy-snow interception dataset #1 (Version 1) [Dataset]. Zenodo. <https://doi.org/10.5281/zenodo.5918637>
- Lundquist, J. D., Currier, W. R., & Baccus, W. (2018). *GPM ground validation snow depth monitoring system OLYMPEx*. NASA Global Hydrology Resource Center DAAC. <https://doi.org/10.5067/GPMGV/OLYMPEx/SNOWTUBE/DATA101>
- Lundquist, J. D., Dickerson-Lange, S., Gutmann, E., Jonas, T., Lumbrazo, C., & Reynolds, D. (2021). Snow interception modeling: Isolated observations have led to many land surface models lacking appropriate temperature sensitivities. *Hydrological Processes*, *35*, e14274. <https://doi.org/10.1002/hyp.14274>
- Lundquist, J. D., Dickerson-Lange, S. E., Lutz, J. A., & Cristea, N. C. (2013). Lower forest density enhances snow retention in regions with warmer winters: A global framework developed from plot-scale observations and modeling. *Water Resources Research*, *49*, 6356–6370. <https://doi.org/10.1002/wrcr.20504>
- Makkonen, L. (2000). Models for the growth of rime, glaze, icicles and wet snow on structures. *Philosophical Transactions: Mathematical, Physical and Engineering Sciences*, *358*(1776), 2913–2939. <https://doi.org/10.1098/rsta.2000.0690>
- Martin, K. A., Van Stan, J. T., Dickerson-Lange, S. E., Lutz, J. A., Berman, J. W., Gersonde, R., & Lundquist, J. D. (2013). Development and testing of a snow interceptometer to quantify canopy water storage and interception processes in the rain/snow transition zone of the North Cascades, Washington, USA. *Water Resources Research*, *49*, 3243–3256. <https://doi.org/10.1002/wrcr.20271>
- Mass, C. F., Albright, M., Ovens, D., Steed, R., MacIver, M., Grit, E., et al. (2003). Regional environmental prediction over the Pacific Northwest. *Bulletin of the American Meteorological Society*, *84*, 1353–1366. <https://doi.org/10.1175/BAMS-84-10-1353>
- Milliman, T. K., Seyednasrollah, B., Young, A. M., Hufkens, K., Friedl, M. A., Frolking, S., et al. (2018). PhenoCam dataset v1.0: Digital camera imagery from the PhenoCam Network, 2000–2015 [Data set]. ORNL DAAC. <https://doi.org/10.3334/ORNLDAAAC/1560>
- Mlawer, E. J., Taubman, S. J., Brown, P. D., Iacono, M. J., & Clough, S. A. (1997). Radiative transfer for inhomogeneous atmospheres: RRTM, a validated correlated-k model for the longwave. *Journal of Geophysical Research*, *102*, 16663–16682. <https://doi.org/10.1029/97JD00237>
- Molotch, N. P., Blanken, P. D., Williams, M. W., Turnipseed, A. A., Monson, R. K., & Margulis, S. A. (2007). Estimating sublimation of intercepted and sub-canopy snow using eddy covariance systems. *Hydrological Processes*, *21*, 1567–1575. <https://doi.org/10.1002/hyp>
- Montesi, J., Elder, K., Schmidt, R. A., & Davis, R. (2004). Sublimation of intercepted snow within a subalpine forest canopy at two elevations. *Journal of Hydrometeorology*, *5*, 763–773. [https://doi.org/10.1175/1525-7541\(2004\)005<0763:SOISWA>2.0.CO;2](https://doi.org/10.1175/1525-7541(2004)005<0763:SOISWA>2.0.CO;2)
- Myhre, G., Plattner, G.-K., Tignor, M. M. B., Allen, S. K., Boschung, J., Nauels, A., et al. (2013). *Climate change 2013: The physical science basis*. In T. F. Stocker, D. Qin, G.-K. Plattner, M. M. B. Tignor, S. K. Allen, J. Boschung, et al. (Eds.), Cambridge University Press. Retrieved from www.cambridge.org
- Niu, G. Y., & Yang, Z. L. (2004). Effects of vegetation canopy processes on snow surface energy and mass balances. *Journal of Geophysical Research*, *109*, D23111. <https://doi.org/10.1029/2004JD004884>
- Olson, D. L., & Delen, D. (2008). Advanced data mining techniques. In *Advanced data mining techniques*. Springer. <https://doi.org/10.1007/978-3-540-76917-0>
- Raleigh, M. S., Currier, W. R., Lundquist, J. D., Houser, P., & Hiemstra, C. (2022). SnowEx17 time-lapse Imagery, version 1 [Data set]. NASA National Snow and Ice Data Center Distributed Active Archive Center. <https://doi.org/10.5067/WYRNU50R9L5R>
- Roesch, A., Wild, M., Gilgen, H., & Ohmura, A. (2001). A new snow cover fraction parametrization for the ECHAM4 GCM. *Climate Dynamics*, *17*, 933–946. <https://doi.org/10.1007/s003820100153>
- Schmidt, R. A., & Gluns, D. R. (1991). Snowfall interception on branches of three conifer species. *Canadian Journal of Forest Research*, *21*, 1262–1269. <https://doi.org/10.1139/x91-176>
- Skamarock, W. C., Klemp, J. B., Dudhia, J., Gill, D. O., Barker, D., Duda, M. G., et al. (2008). *A description of the Advanced Research WRF version 3*. NCAR Tech Note NCAR/TN-4751STR (p. 113). <https://doi.org/10.5065/D68S4MVH>
- Skiles, S. M. K., Flanner, M., Cook, J. M., Dumont, M., & Painter, T. H. (2018). Radiative forcing by light-absorbing particles in snow. *Nature Climate Change*, *8*(11), 964–971. <https://doi.org/10.1038/s41558-018-0296-5>
- Storck, P. (2000). *Trees, snow and flooding: An investigation of forest canopy effects on snow accumulation and melt at the plot and watershed scales in the Pacific Northwest*. Retrieved from <http://fir.library.oregonstate.edu/xmlui/handle/1957/5136>
- Storck, P., Lettenmaier, D. P., & Bolton, S. M. (2002). Measurement of snow interception and canopy effects on snow accumulation and melt in a mountainous maritime climate, Oregon, United States. *Water Resources Research*, *38*(11), 51–516. <https://doi.org/10.1029/2002WR001281>
- Thackeray, C. W., Fletcher, C. G., & Derksen, C. (2014). Seasonal variation of ozone in the tropical lower stratosphere: Southern tropics are different from northern tropics. *Journal of Geophysical Research: Atmospheres*, *119*, 6196–6206. <https://doi.org/10.1002/2013JD021294>
- Thompson, G., Field, P. R., Rasmussen, R. M., & Hall, W. D. (2008). Explicit forecasts of winter precipitation using an improved bulk microphysics scheme. Part II: Implementation of a new snow parameterization. *Monthly Weather Review*, *136*(12), 5095–5115. <https://doi.org/10.1175/2008MWR2387.1>
- Webster, C., & Jonas, T. (2018). Influence of canopy shading and snow coverage on effective albedo in a snow-dominated evergreen needleleaf forest. *Remote Sensing of Environment*, *214*, 48–58. <https://doi.org/10.1016/j.rse.2018.05.023>
- Whiteman, C. D., & Garibotti, R. (2013). Rime mushrooms on mountains: Description, formation, and impacts on mountaineering. *Bulletin of the American Meteorological Society*, *94*(9), 1319–1327. <https://doi.org/10.1175/BAMS-D-12-00167.1>